Diabetes-Associated Mutations in Insulin: Consecutive Residues in the B Chain Contact Distinct Domains of the Insulin Receptor[†,‡]

Bin Xu,[§] Shi-Quan Hu,[||] Ying-Chi Chu,[||] Kun Huang,[§] Satoe H. Nakagawa,[⊥] Jonathan Whittaker,[§,▽] Panayotis G. Katsoyannis,[||] and Michael A. Weiss*[,§]

Department of Biochemistry, School of Medicine, Case Western Reserve University, Cleveland, Ohio 44106-4935, Department of Pharmacology and Biological Chemistry, Mt. Sinai School of Medicine of New York University, New York, New York 10029, Department of Biochemistry and Molecular Biology, The University of Chicago, Chicago, Illinois 60637, and Department of Nutrition, School of Medicine, Case Western Reserve University, Cleveland, Ohio 44106-4906

Received January 30, 2004; Revised Manuscript Received April 8, 2004

ABSTRACT: How insulin binds to and activates the insulin receptor has long been the subject of speculation. Of particular interest are invariant phenylalanine residues at consecutive positions in the B chain (residues B24 and B25). Sites of mutation causing diabetes mellitus, these residues occupy opposite structural environments: Phe^{B25} projects from the surface of insulin, whereas Phe^{B24} packs against the core. Despite these differences, site-specific cross-linking suggests that each contacts the insulin receptor. Photoactivatable derivatives of insulin containing respective *p*-azidophenylalanine substitutions at positions B24 and B25 were synthesized in an engineered monomer (DKP-insulin). On ultraviolet irradiation each derivative cross-links efficiently to the receptor. Packing of Phe^{B24} at the receptor interface (rather than against the core of the hormone) may require a conformational change in the B chain. Sites of cross-linking in the receptor were mapped to domains by Western blot. Remarkably, whereas B25 cross-links to the C-terminal domain of the α subunit in accord with previous studies (Kurose, T., et al. (1994) *J. Biol. Chem. 269*, 29190−29197), the probe at B24 cross-links to its N-terminal domain (the L1 β-helix). Our results demonstrate that consecutive residues in insulin contact widely separated sequences in the receptor and in turn suggest a revised interpretation of electron-microscopic images of the complex. By tethering the N- and C-terminal domains of the extracellular α subunit, insulin is proposed to stabilize an active conformation of the disulfide-linked transmembrane tyrosine kinase.

The biological activities of insulin are mediated by binding of the hormone to receptors on target cells (*1*). Insulin is a globular protein containing two chains, A (21 residues) and B (30 residues). Stored in the pancreatic β cell as a zinc-stabilized hexamer, insulin functions in the blood stream as a zinc-free monomer. The structure of the free hormone has been extensively characterized as a dimer and hexamer by X-ray crystallography (Figure 1A; *2*−*5*).[1] Complementary NMR studies of engineered monomers have demonstrated that major features of such structures are retained in solution (Figure 2A; *6*−*8*). The insulin receptor (IR) comprises two extracellular α subunits and two transmembrane β subunits (Figure 3A,B; for a review, see ref *9*). Binding of insulin to the α subunits activates the tyrosine kinase activity of the cytoplasmic domains of the β subunits, which leads in turn to a cascade of signal-transduction events. Here, we demonstrate by residue-specific photo-cross-linking (*10*) that consecutive residues in the B chain—each a site of mutation causing diabetes mellitus (*11*)—contact distinct domains of the IR. Implications for the mechanism of transmembrane signaling are discussed.

Despite decades of investigation, how insulin binds to and activates the IR is not well understood. The present study is motivated by anomalous structure−activity relationships in the B chain (*12*−*14*). Our approach highlights similarities and differences between Phe^{B24} and its neighboring residue Phe^{B25}. Invariant among vertebrate insulin sequences (Figure

[†] This work was supported in part by the Diabetes Research & Training Center at the University of Chicago (S.H.N.) and by grants from the National Institutes of Health to P.G.K. (DK56673) and M.A.W. (DK40949).

[‡] This paper is dedicated to the memory of the late Howard S. Tager.

* To whom correspondence should be addressed. E-mail: michael.weiss@case.edu. Phone: (216) 368-5991. Fax: (216) 368-3419.

[§] Department of Biochemistry, School of Medicine, Case Western Reserve University.

[||] Mt. Sinai School of Medicine of New York University.

[⊥] The University of Chicago.

[▽] Department of Nutrition, School of Medicine, Case Western Reserve University.

[1] Crystal structures of zinc−insulin hexamers define three alterative conformations: T_6, $T_3R^f_3$, and R_6 hexamers (*2*, *4*, *49*). The solution structure of an engineered insulin monomer (Figure 2A) resembles the crystallographic T-state protomer (*7*, *8*).

[2] Abbreviations: Aib, α-aminoisobutyric acid; CR, cysteine-rich domain of the receptor α subunit; DTT, dithiothreitol; EM, electron microscopy; IGF-I, insulin-like growth factor I; IR, insulin receptor; IRα-N, polyclonal antibody that recognizes 20 amino-terminal residues of the α subunit; kDa, kilodalton (unit of mass); NAv, NeutrAvidin; Pap, *p*-azido-Phe; Pmp, *p*-amino-Phe; UV, ultraviolet; WGA, wheat-germ agglutinin. Amino acids are designated by standard three- and one-letter codes. "Native" elements of structure designate features of crystal structures (*3*) and may not correspond to the functional conformation in a receptor complex (*22*).

10.1021/bi0497796 CCC: $27.50
Published on Web 06/08/2004

A

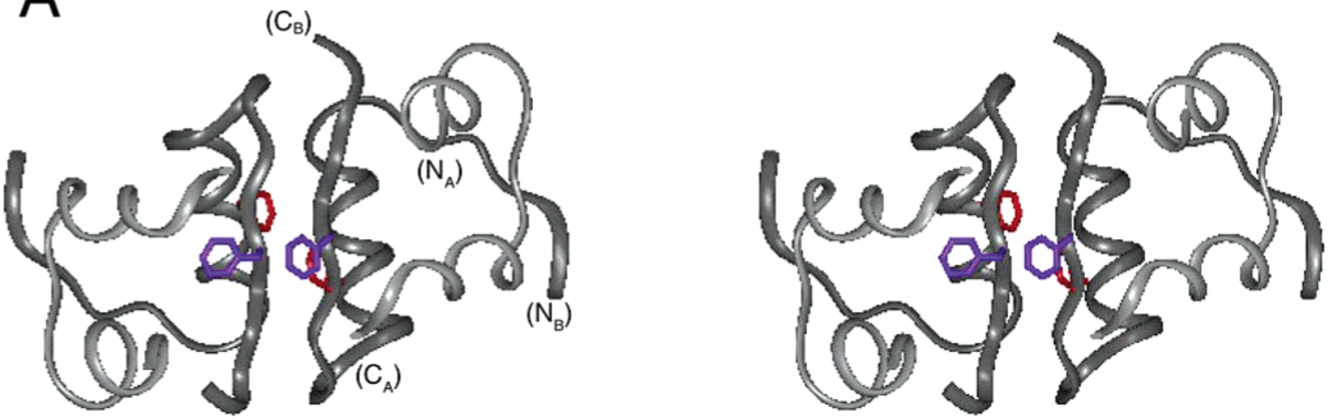

B

										(D)														S	L			(K)	(P)		
human,pig		F	V	N	Q	H	L	**C**	G	S	H	L	V	E	A	L	Y	L	V	**C**	G	E	R	G	F	F	Y	T	P	K	T(A)
cattle		F	V	N	Q	H	L	**C**	G	S	H	L	V	E	A	L	Y	L	V	**C**	G	E	R	G	F	F	Y	T	P	K	A
sheep		F	V	N	Q	H	L	**C**	G	S	H	L	V	E	A	L	Y	L	V	**C**	G	E	R	G	F	F	Y	T	P	K	A
horse		F	V	N	Q	H	L	**C**	G	S	H	L	V	E	A	L	Y	L	V	**C**	G	E	R	G	F	F	Y	T	P	K	A
whale		F	V	N	Q	H	L	**C**	G	S	H	L	V	E	A	L	Y	L	V	**C**	G	E	R	G	F	F	Y	T	P	K	A
rat		F	V	K	Q	H	L	**C**	G	P	H	L	V	E	A	L	Y	L	V	**C**	G	E	R	G	F	F	Y	T	P	K	S
elephant		F	V	N	Q	H	L	**C**	G	S	H	L	V	E	A	L	Y	L	V	**C**	G	E	R	G	F	F	Y	T	P	K	T
guinea pig		F	V	S	R	H	L	**C**	G	S	N	L	V	E	A	T	Y	S	V	**C**	E	D	D	G	F	F	Y	I	P	K	D
Coypu hystricomorphs		Y	V	S	Q	R	L	**C**	G	S	Q	L	V	D	T	L	Y	S	V	**C**	R	H	R	G	F	F	Y	R	P	N	D
chinchilla		F	V	N	K	H	L	**C**	G	S	H	L	V	D	A	L	Y	L	V	**C**	G	D	R	G	F	F	Y	N	P	K	-
cod		A	P	P	Q	H	L	**C**	G	S	H	L	V	D	A	L	Y	L	V	**C**	G	D	R	G	F	F	Y	N	P	K	-
angler	V	A	P	A	Q	H	L	**C**	G	S	H	L	V	D	A	L	Y	L	V	**C**	G	D	R	G	F	F	Y	N	P	K	-
tuna	V	A	P	P	Q	H	L	**C**	G	S	H	L	V	D	A	L	Y	L	V	**C**	G	D	R	G	F	F	Y	N	P	K	-
toadfish 2		A	P	P	Q	H	L	**C**	G	S	H	L	V	D	A	L	Y	L	V	**C**	G	D	R	G	F	F	Y	N	S	-	-
toadfish 1		A	P	P	Q	H	L	**C**	G	S	H	L	V	D	A	L	Y	L	V	**C**	G	D	R	G	F	F	Y	N	P	K	-
bonito		A	A	N	P	H	L	**C**	G	S	H	L	V	E	A	L	Y	L	V	**C**	G	E	R	G	F	F	Y	Q	P	K	T
hagfish		R	T	T	G	H	L	**C**	G	K	D	L	V	D	A	L	Y	I	A	**C**	G	V	R	G	F	F	Y	D	P	T	K M
silver carp		G	A	P	Q	H	L	**C**	G	S	H	L	V	D	A	L	Y	L	V	**C**	G	D	R	G	F	F	Y	T	P	K	T
turkey		A	A	N	Q	H	L	**C**	G	S	H	L	V	E	A	L	Y	L	V	**C**	G	E	R	G	F	F	Y	S	P	T	T
duck, goose		A	A	N	Q	H	L	**C**	G	S	H	L	V	E	A	L	Y	L	V	**C**	G	E	R	G	F	F	Y	S	P	K	T
snake		A	P	N	Q	R	L	**C**	G	S	H	L	V	E	A	L	F	L	I	**C**	G	E	R	G	F	F	Y	S	P	R	T

FIGURE 1: Structure of insulin and sequence conservation of the B chain. (A) Ribbon model of native insulin dimer (*3*). The A chain is shown in light gray and the B chain in dark gray. Residues B24 and B25, sites of present photo-cross-linking, are as indicated: packed against the core of a protomer (B24) and engaged at the dimer interface (B24 and B25). Coordinates were in each case obtained from the Protein Databank: T_6 hexamer (4INS). (B) Sequences of insulin B chains. Invariant positions B24 (red) and B25 (purple) are boxed. Diabetes-associated mutations $Phe^{B24} \rightarrow$ Ser and $Phe^{B25} \rightarrow$ Leu (11) are shown above the top sequence; shown in parentheses are the three substitutions in DKP-insulin that prevent its self-assembly ($His^{B10} \rightarrow$ Asp, $Pro^{B28} \rightarrow$ Lys, and $Lys^{B29} \rightarrow$ Pro; *34*). The structure of DKP-insulin is shown in Figure 2.

1B), these residues occupy different structural environments: Phe^{B25} projects from the surface of an insulin monomer (Figure 2A), whereas Phe^{B24} packs against its core (Figure 2B). Although one edge of the B24 ring is exposed (Figure 2C), predicted solvent accessibilities among crystallographic protomers and NMR models range from 14% to 19%. Structure−activity relationships at B25 are straightforward: a strong preference is observed for aromatic rings (including nonstandard side chains sharing an sp^2-hybridized trigonal carbon at the γ position of the side chain; *15*), suggesting that Phe^{B25} docks against an extended flat nonpolar surface. Aliphatic substitutions, including the diabetes-associated variant $Phe^{B25} \rightarrow$ Leu (designated *insulin Chicago*),[3] markedly impair receptor binding (Table 1B; *16*−*18*). Photo-cross-linking studies of B25 derivatives have established a direct contact to the IR (*10*, *19*). The site of cross-linking has been mapped to the aromatic-rich carboxy-terminal tail of the α subunit (*10*). Structure−activity relationships at B24 are by contrast enigmatic. As at B25, receptor binding is impaired by nonaromatic substitutions (Table 1A; *17*), including diabetes-associated variant $Phe^{B24} \rightarrow$ Ser (*insulin Los Angeles*; *11*). As a seeming paradox, however, Gly^{B24} analogues exhibit near-native activity, and diverse D-amino acid substitutions enhance activity (*12*, *18*, *20*). It is not known whether Phe^{B24} functions to stabilize the structure of insulin, provides a site of main-chain conformational change on receptor binding, or itself contacts the IR. We and others have hypothesized that on receptor

[3] Clinical insulin variants are designated by the location of the original family by analogy to nomenclature describing abnormal hemoglobins (*11*).

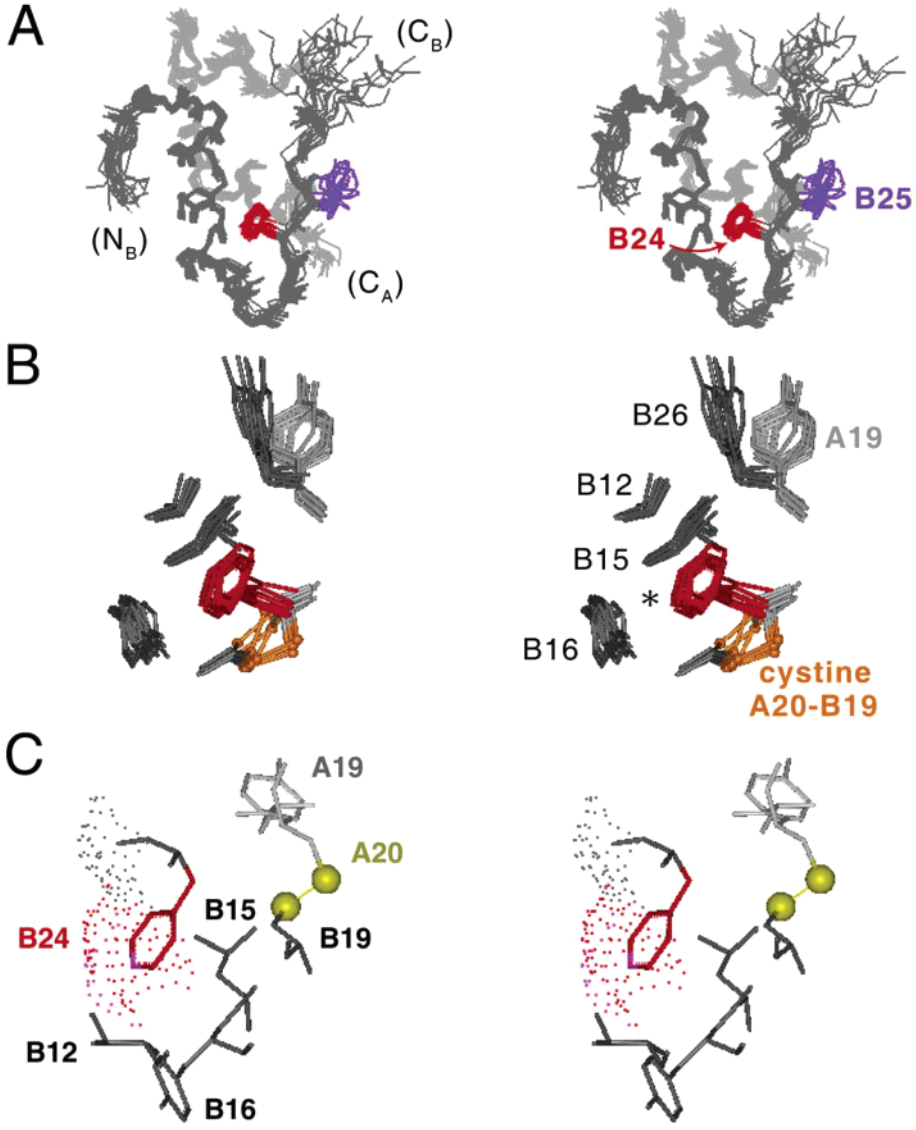

FIGURE 2: Solution structure of an engineered insulin monomer (DKP-insulin; *9*). (A) Phe^{B24} packs against the core, whereas Phe^{B25} is less well ordered on the protein surface. The coloring scheme is otherwise as in (A). (B) Packing scheme of Phe^{B24} in the solution structure of DKP-insulin. Neighboring side chains Val^{B12}, Leu^{B15}, Tyr^{B16}, Cys^{B19}, Tyr^{B26}, Tyr^{A19}, and Cys^{A20} are shown. Sulfur atoms in the disulfide bridge are shown in gold; the coloring scheme is otherwise as in (A). Coordinates were obtained from the Protein Databank: DKP-insulin (1LNP). (C) Dot-surface representation illustrating the partial exposure of the ring of Phe^{B24} (red) as packed against the core. Predicted side chain solvent accessibilities range from 14% to 19%, but the *p*-azido moiety would be expected to extend into the solvent. The structure shown is from molecule 1 of the T_6 zinc hexamer (*3*).

binding the carboxy-terminal segment of the B chain reorganizes to expose a hidden functional surface comprising Phe^{B24} and part of the A chain (*13*, *21*, *22*).

In this paper we exploit site-specific insulin cross-linking to demonstrate that Phe^{B24}, like Phe^{B25}, contacts the IR. Experimental design employs *p*-azidophenylalanine (Pap) as a nearly isosteric substitution for Phe (Figure 3C; *23*). Remarkably, these probes cross-link to noncontiguous sequences in the α subunit: Pap^{B24} cross-links to the amino-terminal domain of the α subunit (the L1 *β*-helix), whereas Pap^{B25} cross-links to its carboxy-terminal region (*10*). Because consecutive residues in insulin contact sites distantly spaced in the sequence of the α subunit, the amino- and carboxy-terminal domains must be close to each other in the hormone−receptor complex. Although surprising, these results are broadly consistent with prior photo-cross-linking studies of insulin derivatized at the *ϵ*-amino group of Lys^{B29} (*24*), effects of receptor mutations on the binding of insulin analogues (*25*), and protein engineering studies of monomeric minimized receptor constructs (*26*). Implications for models of the IR and possible mechanisms of insulin binding (*27*−*32*) are discussed. Together, our results and their structural implications demonstrate the novel utility of contiguous photoactive probes as a molecular ruler.

MATERIALS AND METHODS

Materials. Human insulin was provided by Eli Lilly and Co. (Indianapolis, IN). *tert*-Butoxycarbonylamino acids and derivatives were obtained from Bachem Inc. 4-Methylbenzhydrylamine resin (0.63 mmol of amine/g; Star Biochemicals, Inc.) was used as the solid support for synthesis of the A chain; (*N*-butoxycarbonyl,*O*-benzyl)threonine-phenylacetamidomethyl (PAM) resin (0.6 mmol/g; Bachem, Inc.) was used as the solid support for syntheses of B-chain analogues. Amino acid analyses of synthetic chains and insulin analogues were performed after acid hydrolysis with a Hewlett-

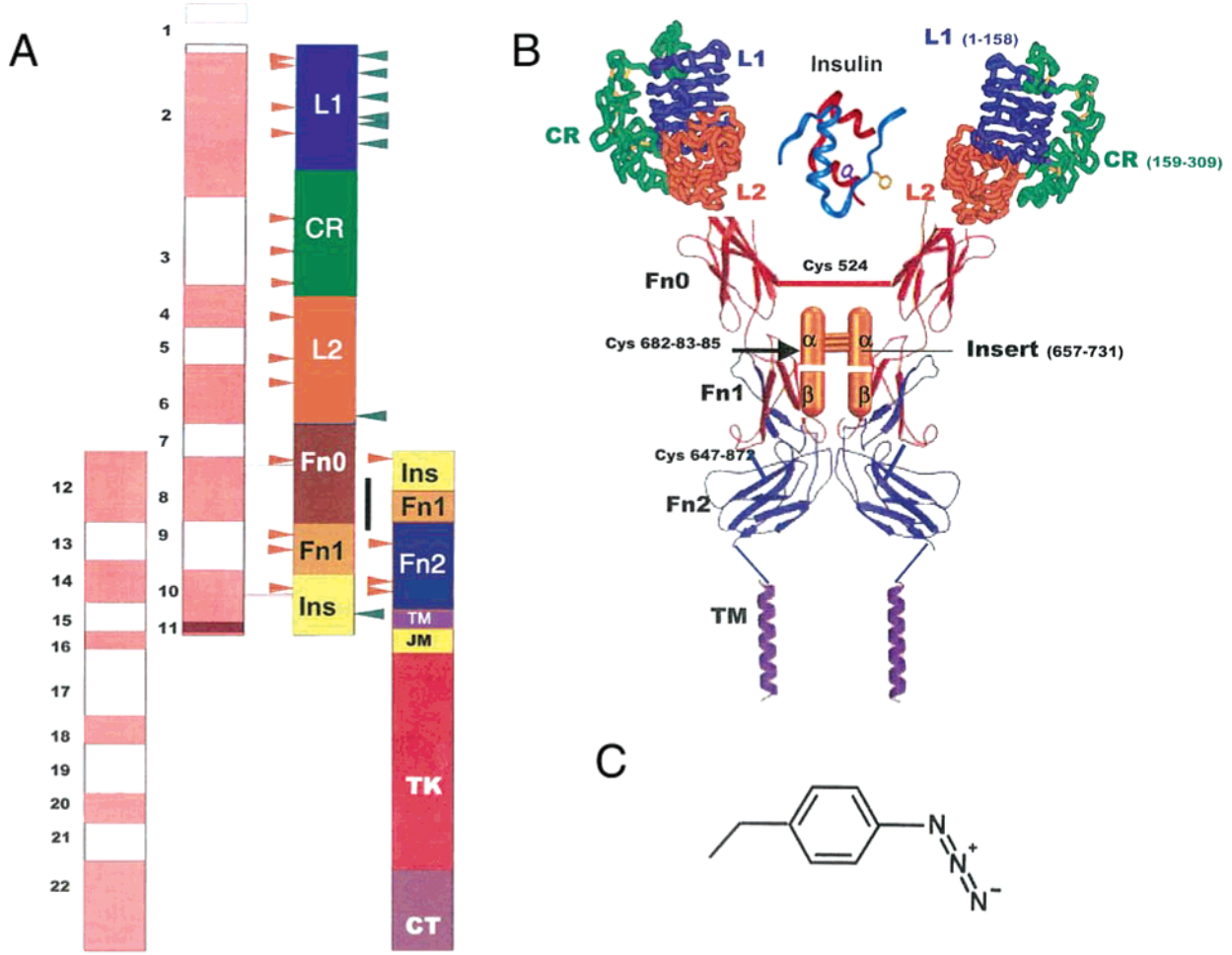

FIGURE 3: Structures of the insulin receptor and *p*-azidophenylalanine. (A, B). Modular structural domains of insulin receptor (adapted with permission from ref *9*). (A) Cartoon of the $\alpha_2\beta_2$ structure of the IR. The left half of the diagram shows boundaries of the regions encoded by the 22 exons of the IR gene. The right half of the diagram outlines predicted boundaries of protein modules. Orange arrowheads indicate N-glycosylation sites. Green arrowheads indicate ligand-binding "hot spots" that have been identified by site-directed mutagenesis (*9*, *46*, *71*). (B) Supradomain organization of the IR (*72*), depicting a "stretched-out" schematic representation of predicted or actual modular structures. The intracellular tyrosine kinase domain is not shown. Residue numbers at boundaries of L1, CR, and insert domains are indicated. A ribbon model of insulin (T state; PDB entry 4INS) is also shown (not to scale); the A chain is shown in red and the B chain in blue. Phe^{B24} (purple) and Phe^{B25} (orange) side chains are shown as sticks. (C) Chemical structure of *p*-azidophenylalanine. Only the side chain of this amino acid analogue is shown.

Packard Amino Quant analyzer (model 1090). Chromatography resins were preswollen microgranular carboxymethylcellulose (CM-cellulose; Whatman CM52), DE52 cellulose (Whatman), and Cellex E (Ecteola cellulose; Sigma); solvents were HPLC grade.

Chemical Syntheses of Insulin Analogues. The protocol for solid-phase synthesis is as described (*33*).

(i) Synthesis of the A Chain. The carboxy-terminal Asn in the synthesis of A-chain analogues was incorporated into the solid support by coupling *tert*-butoxycarbonylaspartic acid α-benzyl ester with 4-methylbenzhydrylamine resin. After the final deprotection, the Asp residue was converted to an Asn residue. Synthesis of A-chain tetra-S-sulfonate was performed as described (*34*). Isolated A-chain tetra-S-sulfonate derivatives were also obtained by oxidative sulfitolysis of human insulin followed by separation of S-sulfonated A and B chains as described (*34*).

(ii) Syntheses of Modified B Chains. B-chain analogues each contain three "DKP" substitutions to prevent self-association of insulin (His^{B10} → Asp, Pro^{B28} → Lys, and Lys^{B29} → Pro; *8*, *35*). Syntheses of DKP-B-chain analogues containing *p*-amino-Phe (at B24 or B25) and 6-biotinyl-amidocaproyl-Phe^{B1} were performed by a modification of the procedure of Kurose and colleagues (*10*). In brief, the *p*-amino-Phe side chain was protected by a 2-chlorobenzyl-oxycarbonyl group. ϵ-Aminocaproyl and biotinyl moieties were incorporated successively at the amino terminus of the 30-residue peptidyl resin by reaction with (a) preformed 1-hydroxybenzotriazole ester in 3-fold excess, (b) N^{ϵ}-*tert*-butoxycarbonylaminocaproic acid, and (c) biotin. The latter active esters were prepared from their respective carboxyl components upon reaction with 1-hydroxylbenzotriazole and *N*,*N*′-diisopropylcarbodiimide. From 0.5 g of the *N*-*tert*-butoxycarbonyl-*O*-benzylthreonine-PAM resin, approximately 2 g of each protected peptidyl resin was obtained; following deblocking and sulfitolysis, crude B-chain derivatives were obtained with an apparent yield of ca. 40% (by weight per gram of peptidyl resin). B-chain analogues were purified by DE-52 cellulose chromatography with apparent yields of 25−30% (by weight per gram of crude peptide).

(iii) Syntheses of Insulin Analogues. Chain combination was effected by interaction of the S-sulfonated derivative of

Table 1: Relative Receptor-Binding Affinities of Selected Insulin Analogues[a]

protein	activity	protein	activity
	A. B24 Analogues		
human insulin	100	[D-Tyr^{B24},L-Phe ^{B26}]-insulin[c]	163 ± 10 (3)
DKP-insulin	161 ± 19 (4)	[Ala^{B24}]-insulin[b]	1.0 ± 0.1 (2)
t_B-DKP-insulin	132 ± 5 (3)	[Gly^{B24}]-insulin[b,d]	78 ± 11 (6)
Pmp^{B24}-t_B-DKP-insulin	59 ± 2 (3)	[Leu^{B24}]-insulin[e,f]	10
[D-Ala^{B24}]-in sulin[b]	150 ± 9 (3)	[Ser^{B24}]-insulin[g,h]	7.0 (3)
[D-Phe^{B24}]-in sulin[b]	140 ± 9 (3)	[Tyr^{B24},Phe^{B26}]-insulin[c]	2.0 ± 0.2 (3)
	B. B25 Analogues		
human insulin	100	[Gly^{B25}]-insulin[b]	1.5 ± 0.3 (3)
DKP-insulin	161 ± 19 (4)	[Leu^{B25}]-insulin[f,j,k]	1−2
t_B-DKP-insulin	132 ± 5 (3)	[Ser^{B25}]-insulin[k]	1.3
Pmp^{B25}-t_B-DKP-insulin	147 ± 3 (3)	[Tyr^{B25}]-insulin[i]	103 ± 11
[Pmp^{B25},Ala^{B29}]-insulin[i]	66 ± 7	[Tyr^{B25},Phe^{B26}]-insulin[c]	82 ± 7 (3)
[D-Tyr^{B25},L-Phe^{B26}]-insulin[c]	0.10 ± 0.01 (2)	Nal(2)^{B25}-insulin[k]	50
[Ala^{B25}]-insulin[g]	7.0 (2)	Nal(1)^{B25}-insulin[k]	24

[a] Pmp analogues each contain biotinylamidocaproyl tagged to the α-amino group of B1 (t_B). [b] Data were obtained from ref *12*. [c] Data were obtained from ref *20*. It is possible that this value is an underestimate (S.H.N., personal communication). [d] An affinity of 22% of insulin was also reported (*18*). [e] Data were obtained from ref *16*. [f] Data were obtained from ref *67*. A related double-mutant analogue [Leu^{B24},Leu^{B25}]-insulin has an affinity of 0.4% (*68*). [g] Data were obtained from ref *18*. [h] Affinities in the range of 0.7−3% were also reported (*69*). [i] Data were obtained fom refs *15* and *17*. [j] Data were obtained from ref *70*. [k] Data were obtained fom ref *17*. The receptor binding affinity and biopotency of depsi-insulin ([B24−B25 CO−O]-insulin)—an insulin analogue with native sequence but substitution of the main-chain peptide bond by an ester—are decreased to 1.7% and 3.5%, respectively (*55*). Abbreviations: Nal(2), L-3-(2′-naphthyl)alanine; Nal(1), L-3-(1′-naphthyl)alanine. Pmp, *p*-aminophenylalanine.

the A chain (40 mg) and B-chain analogue (20 mg) in 0.1 M glycine buffer (pH 10.6, 10 mL) in the presence of dithiothreitol (7 mg) (*8*, *34*). CM-52 cellulose chromatography of each combination mixture enabled partial isolation of the hydrochloride form of the protein contaminated by free B chain. Final purification was accomplished by rp-HPLC. Predicted molecular masses were in each case verified by electrospray mass spectrometry. Final yields were lower than those obtained in a control synthesis of DKP-insulin. For *p*-amino-Phe- and biotin-modified analogues, relative yields were in the range 15−20%.

(iv) Preparation of p-Azido-Phe Derivatives. An ice-cold solution of the corresponding *p*-amino-Phe analogue of DKP-insulin (3 mg; described above) dissolved in 0.4 mL of 0.1 N HCl was treated in the dark with 15 μL of 0.5 M $NaNO_2$ solution. After being stirred on ice for 15 min, the reaction mixture was treated with 75 μl of 0.1 M sodium azide, stirred further for 30 m, and diluted with 5 mL of saturated picric acid solution. The precipitated picric acid salt of the analogue was isolated and converted to the hydrochoride. Purification of the analogue by rp-HPLC gave the purified *p*-azido-Phe derivative in 30−35% yield. A photostable analogue of DKP-insulin containing Phe at B24 and B25 with a biotin tag at B1 was likewise prepared as a control. All procedures were performed in dim light. Predicted changes in molecular mass were verified by electrospray mass spectrometry.

Insulin Binding Assays. To verify the activities of *p*-amino-Phe-substituted and biotin-modified analogues prior to photocross-linking studies of the corresponding *p*-azido-Phe derivatives, a human placental membrane preparation containing the IR was employed as described (*36*). Membrane fragments (0.025 mg of protein/tube) were incubated with ^{125}I-labeled insulin (ca. 30000 cpm) in the presence of selected concentrations of unlabeled peptide for 18 h at 4 °C in a final volume of 0.25 mL of 0.05 M Tris−HCl and 0.25% (w/v) bovine serum albumin at pH 8. After incubation, each mixture was diluted with 1 mL of ice-cold buffer and centrifuged (10000*g*) for 5 min at 4 °C. The supernatant was then removed by aspiration, and the membrane pellet counted for radioactivity. Data were corrected for nonspecific binding (amount of radioactivity remaining membrane-associated in the presence of 1 μM human insulin). The relative activity is defined as the ratio of analogue to human insulin required to displace 50% of specifically bound ^{125}I-labeled human insulin (Amersham). In all assays the percentage of tracer bound in the absence of competing ligand was less than 15% to avoid ligand-depletion artifacts.

Cell Culture. A stably transfected dihydrofolate-deficient Chinese hamster ovary cell line (DG44) overexpressing human insulin receptor, P3-A (kindly provided by Prof. Donald F. Steiner, HHMI and The University of Chicago) was cultured in α minimum essential medium along with 100 nM methotrexate containing 10% dialyzed heat-inactivated fetal bovine serum and 1× penicillin/streptomycin (Invitrogen Life Technologies, CA) at 37 °C under 5% CO_2. Confluent cells were detached either by treatment with 1× trypsin−ethylenediaminetetraacetic acid (EDTA) solution (Cellgro, VA) or by Hanks-based enzyme-free cell dissociation buffer (Invitrogen Life Technologies, CA). Cells were collected and washed with ice-cold 1× PBS. Cell pellets were saved at −80 °C.

Insulin Receptor Purification. P3-A cell pellets were solubilized in 1% Triton X-100, 20 mM HEPES (pH 7.8), and 150 mM NaCl containing a protease inhibitor cocktail (Roche, IN) for 30 min at 4 °C. Cell lysates were centrifuged at 20000*g* for 30 min at 4 °C. The supernatant was collected, and the particulate was removed. Glycerol was then added to a final concentration (v/v) of 10%. The cell extract was then incubated with wheat-germ agglutinin-coupled agarose (WGA; Vector Laboratories, CA) on a rotator at 4 °C for 4 h. The resin was then transferred into 15 mL columns (Bio-Rad, CA) and washed once each with 20 mM HEPES (pH 7.8), 150 mM NaCl, 0.1% Triton X-100, and 10% glycerol and 20 mM HEPES (pH 7.8), 500 mM NaCl, 0.1% Triton X-100, and 10% glycerol at 4 °C. The holoreceptor and other glycoproteins were eluted with 20 mM HEPES (pH 7.8), 0.15 M NaCl, 0.1% Triton X-100, 10% glycerol, and 0.3 M *N*-acetyl-glucosamine in 0.5−1 mL fractions. The concentra-

tion of the eluted protein fraction was measured by the Bradford assay (Bio-Rad, CA). Peak fractions were pooled, and receptor purity was evaluated by sodium dodecyl sulfate−polyacrylamide gel electrophoresis (SDS−PAGE) following Commassie Blue staining. Typically, 50−60% pure IR was obtained. Binding was measured with polyethylene glycol-8000 precipitation according to the method of Schäffer (*37*).

Photo-Cross-Linking Studies. To obtain 1:1 hormone−receptor complexes, WGA-purified IRs or the isolated secreted ectodomains were mixed with photoactive insulins labeled at indicated positions at ligand and receptor concentrations of 100−200 nM at 4 °C followed by shaking overnight. The complexes were then transferred to a Costar assay plate (Corning Inc., NY) for UV irradiation. Photo-cross-linking was effected by short-wave ultraviolet irradiation (UV at 254 nm as generated from a Mineralight lamp, model UVG-54; UVP, Upland, CA); optimal parameters were a duration of 20 s and a distance of 1 cm from the light source. After cross-linking and reduction of the complexes by dithiothreitol (100 mM DTT), the solutions were separated by 10−20% gradient SDS−PAGE. The separated proteins were then blotted onto a nitrocellulose membrane. Cross-linked adducts were probed with NeutrAvidin (Pierce Chemicals, Rockford, IL; designated NAv in Figures 5−7). To identify amino-terminal fragments of the α subunit, blots were also probed with polyclonal anti-IRα antibody (catalog number SC-710, Santa Cruz Biotechnology, Santa Cruz, CA). This anti-peptide antibody (designated IRα-N in the figures) recognizes residues 1−20 of the α subunit.

Proteolytic Mapping of Cross-Linking Sites. Sites of cross-linking between Pap derivatives of insulin and the WGA-purified IR were mapped to amino- or carboxy-terminal domains of the α subunit as follows.

(i) Chymotrypsin Digestion. Affinity-purified holoreceptors were photo-cross-linked with photoactivatable insulins labeled at indicated positions as above. Digestion was performed at 37 °C with 100 μg/mL chymotrypsin (Sigma, St. Louis, MO) in 50 mM HEPES (pH 7.4), 0.1% Triton X-100, and 0.11 M NaCl. At the indicated time points the digestion was stopped by heating aliquots at 95 °C for 5 min; an equal volume of Laemmli sample buffer was then added. The solutions were treated with or without 100 mM DTT as described. The digestion mixtures were then separated by a 12.5% SDS−PAGE gel and transferred electrophoretically to a nitrocellulose membrane. Samples were probed with NAv or anti-IRα antibody (IRα-N).

(ii) Trypsin Digestion. WGA-purified holoreceptors were cross-linked with photoactivatable insulins labeled at indicated positions as described above. Digestion was performed at room temperature with 70 μg/mL trypsin supplemented with EDTA (Cellgro, VA) in 50 mM HEPES (pH 7.4), 0.1% Triton X-100, and 0.11 M NaCl. At the indicated time points the digestion was stopped by addition of 200 μg/mL soybean trypsin inhibitor (Sigma, MO), followed immediately by heating at 95 °C for 5 min. An equal volume of Laemmli sample buffer was added, and the solutions were treated with 100 mM DTT. The digestion mixtures were then separated by 10−20% gradient SDS−PAGE and blotting onto a nitrocellulose membrane. Samples were probed with NeutrAvidin or anti-IRα antibody.

Deglycosylation of Insulin Receptor and Tryptic Fragments. Tryptic fragments of the Pap-cross-linked IR complexes were deglycosylated with peptide-*N*-glycosidase F (N-Glycanase; Prozyme, CA). Samples were denatured at 95 °C for 5 min in 20 mM sodium phosphate (pH 7.5) containing 0.1% SDS and 50 mM β-mercaptoethanol prior to deglycosylation. The solutions were cooled to room temperature, and nonionic detergent NP-40 (final concentration 0.75%) and N-Glycanase (1 mU/μg of receptor in the initial tryptic digestion) were added. Samples were incubated at 37 °C for 4 h. The reaction was stopped by heating at 95 °C for 10 min. An equal volume of Laemmli sample buffer was added for SDS−PAGE. Control deglycosylation of the intact α subunit indicated complete conversion of the 135 kDa glycoprotein band to a 98 kDa band in accord with past studies (*38*).

Interpretation of Molecular Masses. The electrophoretic mobility of the B24-cross-linked N-terminal glycosylated tryptic fragment corresponds to a molecular mass of 31 kDa; following enzymatic deglycosylation the apparent mass is 20 kDa (see the Results). Inferred masses in SDS−PAGE analysis of the corresponding unlinked receptor fragment (obtained by analysis of noncovalent IR complexes containing native insulin) are 28 and 17 kDa, respectively. These masses are consistent with the sequence of the L1 domain and its pattern of N-linked glycosylation as follows. The putative structure of the L1−CR−L2 region (as obtained by homology modeling; see below) predicts three prominent tryptic sites at positions K149, K164, and K166. The first site (N**K**DD; residues 148−151) projects from an exposed loop near the C-terminus of the L1 domain (Figure 6C). The following sites (PGTA**K**G**K**TNCP; residues 160−170) project from a loop at the beginning of the CR domain. Cleavage at these sites would yield (in the absence of glycosylation) 17−19 kDa fragments; the tethered B chain would provide an additional 3.7 kDa. An additional 11 kDa (the difference in apparent mass on deglycosylation; see the Results) is attributed to carbohydrate moieties consistent with the three N-linked glycosylation sites in the L1 domain (at residues N16, N25, and N111; the average mass per N-linked glycosylation site in the α subunit is ca. 4 kDa; *39*).

Control Studies of the B25-Cross-Linked Complex. Pap^{B25} has previously been shown to cross-link to residues 704−718 of the α subunit (*10*). To correlate this result with the present mapping strategy, studies of the Pap^{B25} analogue were extended to studies of a pretrypsinized but active receptor. Gentle digestion of the cell-bound IR serendipitously yielded an active derivative containing a carboxy-terminal cleavage about 28 kDa (including glycosylation) from the end of the α subunit. The truncated α subunit (apparent molecular mass about 107 kDa) contains the amino-terminal IRα-N epitope and hence contains the L1 domain (asterisk in Figure 7D). Under native conditions carboxy-terminal fragment(s) are presumably retained within the disulfide-cross-linked $\alpha_2\beta_2$ structure, giving rise to a nativelike assembly able to bind insulin. Although present in both B25 and B24 reaction mixtures, the 107 kDa band cross-links only to the Pap^{B24} analogue (asterisk in Figure 7C, lane 12 versus lane 10). Resolution of this high-molecular-weight band from the native α subunit by low-percentage SDS−PAGE (5% acrylamide) implies a mass difference of 28 kDa (data not shown). Given the glycosylation pattern of the receptor (tan

arrowheads in Figure 3A; *39*), we estimate that the 107 kDa fragment lacks the carboxy-terminal 150−160 residues. Additional mapping information is provided by observation of a smaller domain obtained on further chymotryptic digestion of the B25-cross-linked complex: its mass is 20 kDa (glycosylated) and 17 kDa (deglycosylated; data not shown). On the basis of the results of Steiner and colleagues (*10*), this fragment (ca. 120 residues and containing two glycosylation sites) consists of the α-specific portion of the $FnIII_1$ domain (residues 615−656) and C-terminal tail derived from the insert domain (residues 657−731). It is not known whether the fragment extends to the extreme C-terminus.

Molecular Modeling. A homology model of the L1−CR−L2 region of the IR was constructed on the basis of the crystal structure of the corresponding domain of the IGF receptor (*40*) as described by De Meyts and Whittaker (*9*). The modeling procedure employed the SWISS-MODEL protocol (website http://swissmodel.expasy.org) as described (*41*). The L1−CR−L2 sequences of the IR and IGF receptor exhibit 60% identity and 78% similarity.

RESULTS

Our study has two parts. We first investigated the photo-cross-linking properties of photoactivatable insulin derivatives containing Pap substitutions at position Phe^{B24} or Phe^{B25}. Cross-linking is in each case demonstrated to both the secreted ectodomain of the IR and the lectin-purified holoreceptor. Receptor contact sites were then mapped by limited proteolysis. Chymotryptic and tryptic sites in the α subunit are utilized to assign contacts to amino- and carboxy-terminal domains. The domain organization of the α subunit, inferred from comparative sequence analysis, is as follows: a tripartite amino-terminal region containing two globular L domains flanking a cysteine-rich domain (designated L1−CR−L2) followed by fibronectin-homology regions (FnIII-0 and FnIII-1) and a carboxy-terminal tail derived from the insert domain of the second FnIII domain (FnIII-1; Figure 3).[4]

Pap was chosen on the basis of its rigidity, small size, and resemblance to native phenylalanine (Figure 3C). The photoactivatable side chain was in each case introduced into an engineered insulin monomer (DKP-insulin), which was chosen as a template for its efficiency of synthesis, enhanced receptor binding, and absence of confounding self-association (*8*, *35*). The analogues contain a biotin tag at the α-amino group of the B chain to enable detection of photo-cross-linked fragments by avidin-based reagents. Although photoactive probes at residue B25 have previously been characterized (*10*, *19*), to our knowledge this is the first description of a photoactive probe at B24. Whereas Phe^{B25} projects from the surface of the monomer, Phe^{B24} is largely buried as a structural component at the edge of the hydrophobic core (Figure 2).

I. Photo-Cross-Linking Studies. The photoactivatable derivatives of B24 and B25 were prepared by total chemical synthesis (see the Materials and Methods). Fidelity of synthesis and quantitative conversion of *p*-amino-Phe to Pap was verified in each case by electrospray mass spectrometry. *p*-Amino-Phe-containing precursors each exhibit high affinity for the IR: 59 ± 2% for Pmp^{B24} and 147 ± 3% for Pmp^{B25} (mean and standard deviation of three replicates) relative to native human insulin. Under these conditions, the relative affinity of the corresponding biotin-tagged DKP-insulin, prepared as a control, is 135 ± 10%. A short UV exposure time (20 s) yields essentially complete photolysis or cross-linking. The analogues and receptor were mixed at 1:1 overall stoichiometry at a concentration (ca. 200 nM) more than 100-fold higher than the weakest dissociation constant. Under these conditions the predominant species is expected to be a 1:1 molecular complex, although higher-order hormone−receptor complexes are also possible. Efficient photo-cross-linking is observed to the secreted ectodomain of IR (Figure 4A; *42*) and WGA-purified holoreceptor (Figure 4C). Similar results are obtained at successively higher concentrations of the insulin derivative, demonstrating that the extent of cross-linking is not limited by site occupancy and is independent of possible changes in the stoichiometry of the molecular complexes. Control experiments to verify specificity were performed to demonstrate competition between binding of the Pap analogues and native ligands (human insulin and IGF-I; Figure 4B,D, respectively). Additional control experiments demonstrated that no photo-cross-linking reactions occurred between Pap^{B25} and heterologous proteins (lysozyme and IgG) or between the photostable precusor Pmp^{B25}-DKP-insulin and the ectodomain under the same conditions (data not shown). Addition of a 2−4-fold molar excess of Pap^{B25}-DKP-insulin to the WGA-purified IR did not result in an increased yield of photo-cross-linked α subunit.

II. Mapping Studies. Insulin-binding regions of the IR are contained within its α subunits. Cross-linking studies suggest that sites of contact are distributed among noncontiguous segments of the α polypeptide sequence (*10*, *24*, *43*, *44*). Several models of the quaternary organization of the extracellular IR domains have been proposed on the basis of single-molecule EM images (*27*−*32*). Despite considerable such efforts, atomic-scale interpretation remains unclear.[5]

To identify insulin-binding domains of the receptor α subunit, we exploited domain-specific markers following limited chymotryptic or tryptic digestion of the covalent complexes (Figures 4−7). The essential idea is to distinguish between the L1 domain—previously shown to be a major determinant of insulin binding (*44*−*46*)—and the rest of the α subunit. The L1 domain spans residues 1−157 and folds as a *β*-helix (*40*). A commercial polyclonal antiserum has been raised against a peptide encompassing the 20 amino-terminal residues of this domain (Santa Cruz Biotechnology); this antibody (designated IRα-N in the figures) is suitable for Western blotting. Cross-linked hormone−receptor fragments were likewise visualized by enzyme-enhanced chemiluminescence following blotting with NAv Pierce Chemicals). Apparent molecular masses were inferred in relation

[4] The nomenclature describing the modular domains of the IR is defined as described (*9*, *58*).

[5] The crystal structure of the homologous L1−CR−L2 region of the IGF receptor, determined at 2.6 Å resolution, demonstrates that the L1 and L2 domains (blue and orange in Figure 3B) form *β*-helices (*40*) as depicted in Figure 3B. Although the L1−CR−L2 fragment does not bind IGF-1 or insulin, mutagenesis studies of secreted IGF-I- and IR-derived ectodomains demonstrate that respective L1 domains play major roles in ligand binding (*46*, *74*) in accord with the results of cross-linking (*24*) and analysis of chimeric receptors (*45*, *61*, *63*).

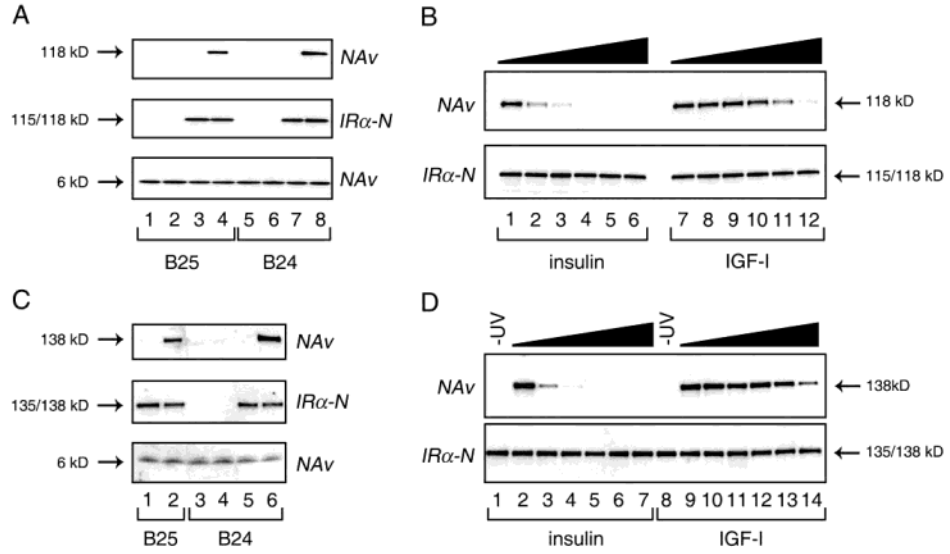

FIGURE 4: Photo-cross-linking of Pap^{B25} and Pap^{B24} to isolated secreted ectodomain (A) or holoreceptor (C) and respective cross-linking control assays (B and D). (A, C) Western blots showing the ectodomain of the IR (panel A, $\alpha_2\beta'_2$, 290 kDa; α, 115 kDa; β', 30 kDa) or holoreceptor (panel C, $\alpha_2\beta_2$, 460 kDa; α, 135 kDa; β, 95 kDa) cross-linked with DKP-insulin containing Pap substituted at either position B25 (lanes 1−4 in panel A and lanes 1−2 in panel C) or position B24 (lanes 5−8 in panel A and lanes 3−6 in panel C) treated without (odd-numbered lanes) or with (even-numbered lanes) UV irradiation. DKP-insulin analogues have a biotin tag at B1. After cross-linking, reduction with DTT (top and middle panels of parts A and C), SDS−PAGE separation, and blotting onto nitrocellulose membranes, cross-linked adducts were probed with alkaline phosphatase conjugated NAv (top panels of parts A and C). Control blots probed by IRα-N (middle panels of parts A and C; after DTT reduction) demonstrate equal amounts of IR. Similarly, control blots probed with NAv (bottom panels of parts A and C; without DTT reduction) demonstrate equal amounts of insulin analogue. (B, D) Competition experiments. Western blots showing photoactive Pap^{B25} binding to receptor competing with increasing amounts of human insulin (or IGF-I) followed by photo-cross-linking and Western blotting analysis; data for the ectodomain are shown in panel B and for the holoreceptor in panel D. Concentrations of the competing ligands (panel B, lanes 1−6 (insulin) and lanes 7−12 (IGF-I)) were successively 0, 6, 20, 60, 200, and 600 times that of Pap^{B25}. The same stoichiometries were employed in panel D (lanes 2−7 (insulin) and 9−14 (IGF-I), respectively). The absence of photo-cross-linking in the absence of UV irradiation are also shown in panel D (lanes 1 and 8).

to standards with and without N-linked glycosylation; there are no O-linked carbohydrates in the α subunit (*39*).

Our initial strategy is based on the previous identification by Pilch and colleagues of a unique amino-terminal 50 kDa chymotryptic fragment of the α subunit (*47*). This glycosylated fragment, which is relatively resistant to further proteolysis (*47*), contains the amino terminus of the α subunit (on the basis of Edman sequencing) and spans the L1 β-helix and most of the CR domain. Parallel Western (IRα-N antiserum) and NAv blotting of chymotryptic digests of the Pap^{B24}-photo-cross-linked complex thus enables visualization of a 50 kDa band indicating photo-cross-linking to the L1−CR region (lanes 5−8 in Figure 5A,B). The identity of this amino-terminal 47 kDa chymotryptic receptor fragment was validated by affinity pull-down using streptravidin-conjugated agarose beads followed by Western blotting with the IRα-N antibody: the same fragment contains both biotin and the L1 epitope (left-hand lanes of Figure 5C,D). Whereas such mapping demonstrates that Pap^{B24}-DKP-insulin cross-links to the amino-terminal fragment, the Pap^{B25} analogue does not (lanes 1−4 in Figure 5A and open box in Figure 5D). Cross-linking of Pap^{B25}-DKP-insulin to sites carboxy-terminal to the L1−CR region is consistent with previous studies (*10*).[6] Control studies of the Pap^{B25}-cross-linked complex are described in the Materials and Methods.

To define further the B24-binding region, we have employed analogous amino-terminal tryptic fragments following limited digestion of the covalent hormone−receptor complex (Figure 6A). A unique amino-terminal 31 kDa cross-linked glycosylated fragment was thus identified in Pap^{B24}-cross-linked complexes (lanes 5−8 in Figure 7A,B) but not in Pap^{B25}-cross-linked complexes (lanes 1−4). Analogous to "supershift" gel assays, both the free L1 domain (28 kDa in the glycosylated form) and cross-linked L1 domain (31 kDa; 3 kDa contributed from the B chain of the photoactive analogue) were observed using amino-terminal α-subunit receptor antisera as the Western probe (Figure 6A). Following enzymatic deglycosylation, the apparent mass of this fragment is 20 kDa (lanes 1 and 2 in Figure 6B); control tryptic digestion of a native insulin−IR complex yields a corresponding 17 kDa N-terminal deglycosylated fragment. The molecular mass of this fragment indicates that it contains about 150 amino acids (given possible electrophoretic anomalies, a conservative upper bound would be fewer than 170 amino acids) and thus consists of the L1 domain. Inspection of the homology model of the L1−CR−L2 domains (Figure 6C) predicts exposed tryptic sites at positions K149, K164, and K166 (red in Figure 6C). Cleavage at K149, within a loop connecting the L1 β-helix to the CR domain, would be most consistent with the mass of the deglycosylated fragment. The difference in mass between the glycosylated and deglycosylated fragments (11 kDa) is consistent with the presence of three N-linked

[6] Steiner and colleagues characterized a Pap^{B25} derivative of the truncated insulin analogue des[B26−B30]-B25-*p*-azidophenylalanine-α-carboxamide-insulin containing a B1 biotin tag. The Pap moiety was found to cross-link to a carboxy-terminal peptide derived from the insert domain (residues 704−718; *10*). Similar results have been obtained with the Pap^{B25} derivative of intact insulin (L. Schäffer, personal communication).

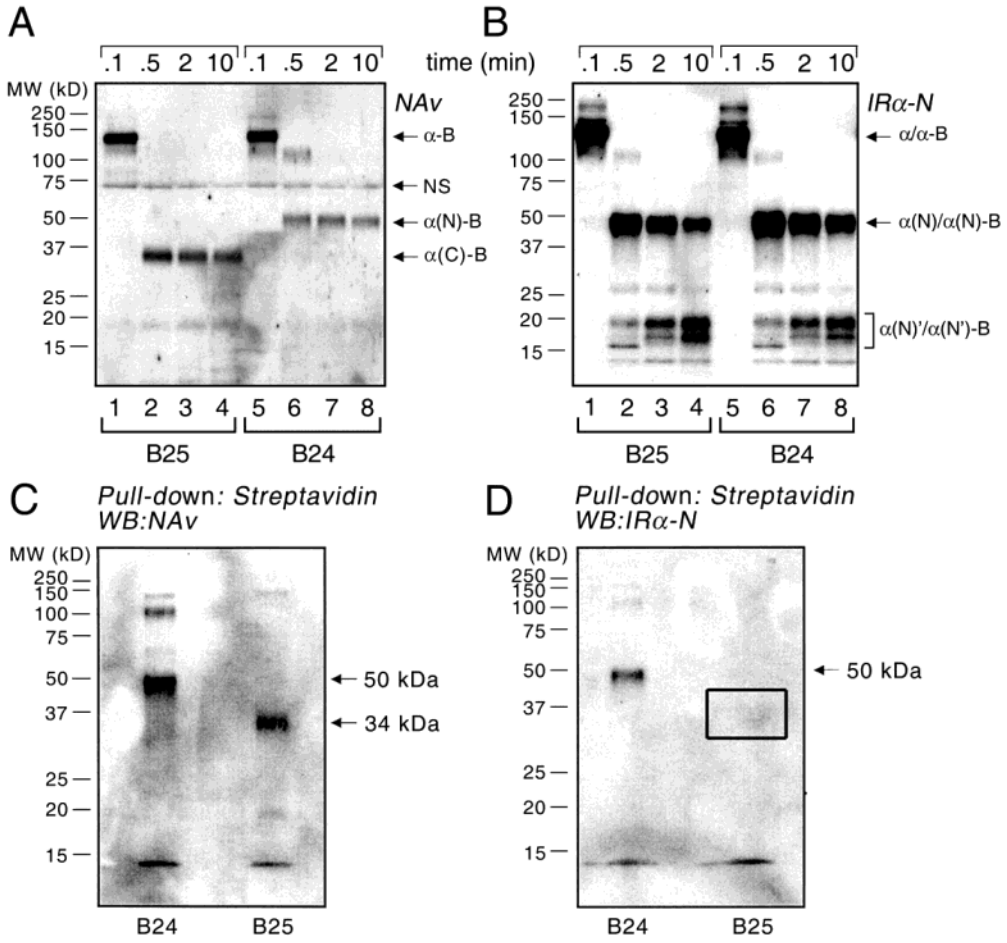

FIGURE 5: Limited chymotrypsin digestion of Pap^{B25}- or Pap^{B24}-cross-linked IR and affinity pull-down assays. (A, B) Affinity-purified holoreceptor was cross-linked to Pap^{B25} or Pap^{B24} derivatives of DKP-insulin and digested with chymotrypsin as described in the Materials and Methods. At indicated time points (top of the gels), aliquots of the digestion mixture were mixed with an equal volume of Laemmli sample buffer containing 100 mM DTT and heated at 95 °C for 5 min. SDS−PAGE gels were probed with alkaline phosphatase conjugated NeutrAvidin (panel A) or anti-IRα antibody (B). Three times as much protein was loaded in lanes 1−4 of panel A as in lanes 5−8. "NS" (panel A) designates nonspecific binding of NAv to a contaminating protein. Positions of molecular weight standards are shown at the left of each gel. (C, D) The Pap^{B24}- or Pap^{B25}-conjugated IR complex was digested with chymotrypsin and mixed with streptavidin-linked agarose beads after reduction by DTT. Unbound receptor fragments were washed away, and bound receptor fragments were eluted by boiling at 90 °C for 15 min in Laemmli sample buffer. Eluted fragments were separated by 12.5% SDS−PAGE and blotted on nitrocellulose membranes. Signals were visualized by either alkaline phosphatase conjugated NeutrAvidin (C) or anti-IRα antibody (D). The empty box in panel B indicates the absence of the 40 kDa band diagnostic of photo-cross-linking of the Pap^{B25} analogue to the carboxy-terminal region of the α subunit. "WB" indicates Western blot; NAv, NeutrAvidin; and IRα-N, anti-peptide antibody recognizing 20 amino-terminal residues of α subunit.

glycosylation sites (see the Materials and Methods; *39*). Absence of this SDS−PAGE fragment without reduction of the tryptic products by DTT is consistent with the presence of interlocking disulfide bridges spanning the candidate tryptic sites (Supporting Information).

Separation of free and cross-linked receptor fragments allows photo-cross-linking efficiency to be estimated on the basis of the relative intensities of these bands. Apparent efficiencies are approximately 20% for both Pap^{B24} and Pap^{B25}; actual effiencies might be even higher since the WGA-purified IR may not be completely active. Because Phe^{B24} and Phe^{B25} are contiguous residues, cross-linking of the corresponding Pap derivatives to different regions of the IR demonstrates that the amino- and carboxy-terminal regions of the α subunit lie in close proximity in the hormone−receptor complex. These results do not indicate whether the proximate domains belong to the same α subunit or lie across a subunit interface of the $\alpha_2\beta_2$ heterotetramer.

DISCUSSION

Binding of insulin to the IR plays a central role in the hormonal control of metabolism (*1*). The present study is motivated by anomalous structure−activity relationships in the insulin B chain. Such anomalies have attracted broad interest in relation to possible mechanisms of binding to the IR. Because insulin exhibits conformational variability among crystal structures (*2*, *4*, *49*, *50*), its active conformation is not well understood. In this paper we have focused on two invariant side chains in the C-terminal β-strand, Phe^{B24} and Phe^{B25}. These conserved residues are of special importance as sites of rare clinical mutations causing diabetes mellitus (*11*), and their roles in receptor binding have been extensively investigated by mutagenesis (*12*, *17*, *20*, *51*). Residue-specific photo-cross-linking studies have previously suggested that Phe^{B25} directly contacts the IR (*10*, *19*). Here, we have extended this approach to Phe^{B24}, a proposed site of conformational change on receptor binding.

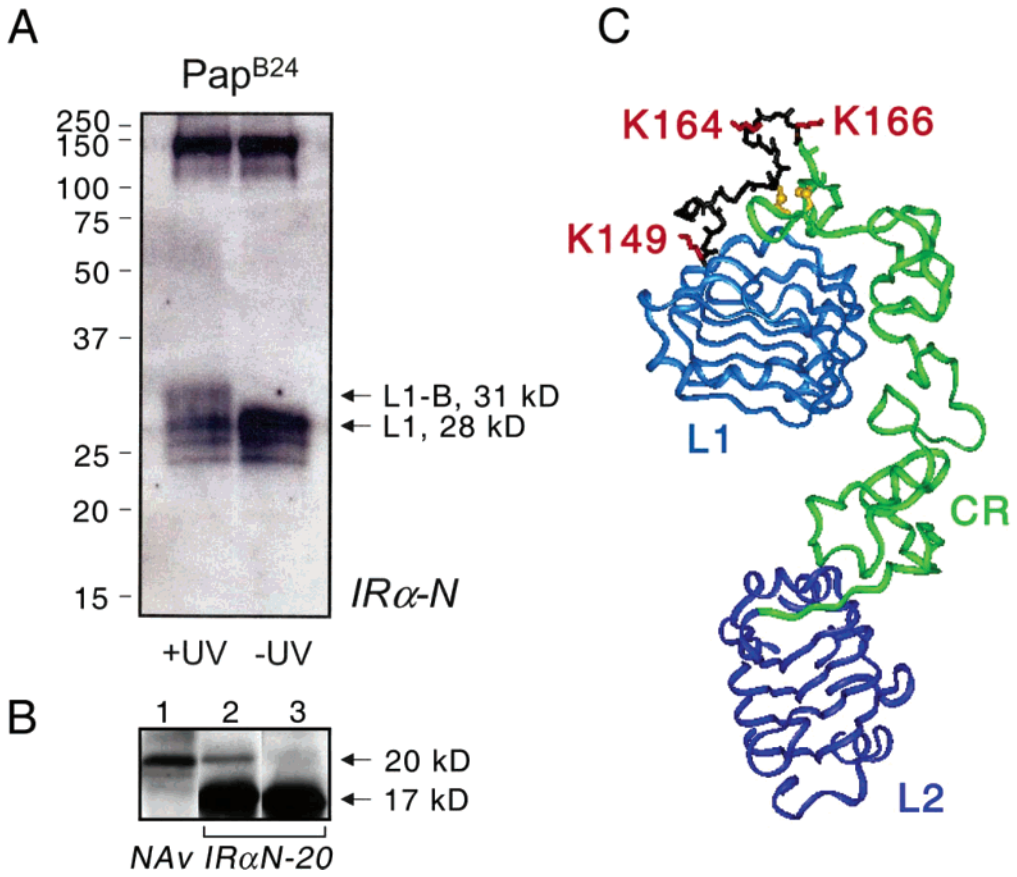

FIGURE 6: Supershift of the cross-linked receptor α fragment and model of L1−CR−L2 domains of the IR. (A) The apparent efficiency of cross-linking is determined by comparison of free and photo-cross-linked receptors. Left-hand lane: WGA-purified IR was cross-linked to the Pap^{B24} derivative of DKP-insulin and digested with trypsin. Right-hand lane: the corresponding digestion of free IR. In each case digestion was stopped after 10 min by adding soybean trypsin inhibitor. Heat-inactivated and denatured aliquots were resolved by SDS−PAGE and visualized by IRα-N. A 12.5% linear resolving SDS−PAGE system was used for optimal separation of 25−40 kDa fragments. (B) Enzymatic deglycosylation of B24-cross-linked tryptic fragments enhances resolution, sensitivity, and accuracy of SDS−PAGE analysis. Lane 1: NAv-detected Western blot demonstrates that above 31 kDa the glycosylated B24-cross-linked fragment runs at 20 kDa following deglycosylation. Lane 2: IRαN-detected Western blot demonstrates a 3 kDa mass difference between B24-cross-linked and native fragments (20 versus 17 kDa). Lane 3: control IRαN blot following tryptic digestion of IR bound to unmodified insulin (i.e., in the absence of Pap probe). (C) Ribbon representation of a homology model of L1−CR−L2 domains of the IR based on the crystal structure of the corresponding domain of the IGF receptor. The modeling procedure employed the SWISS-MODEL protocol as described in the Materials and Methods. The L1 domain is shown in blue, CR in black or green, and L2 in purple. Junctional segments between L1 and CR domains (residues 149−194) are represented as black sticks. Within this sequence, two disulfide bridges (cystines 159−182 and 169−188) are shown in yellow; the disulfide bridge at cystine 126−155 is not shown. Three putative tryptic sites (Lys149, Lys164, and Lys166) are highlighted in red. The sequence of the IR L1−CR−L2 domains is given in the Supporting Information in relation to the sequence of IGF-I.

Does Phe^{B24} Redirect the Main-Chain Configuration of the B-Chain β-Strand? Phe^{B24} occupies a similar environment in all crystal structures of insulin. Stable packing interactions are observed between the aromatic side chain and conserved side chains in the core; van der Waal contacts are observed with Val^{B12}, Leu^{B15}, and the A20−B19 disulfide bridge (*3*, *4*, *50*). These interactions are retained in a monomer in solution (Figure 2B; *6*, *7*, *52*). Phe^{B24} thus seems to provide a key structural support to seal one face of the hydrophobic core. Surprisingly, substitution of Phe^{B24} by glycine does not significantly affect the affinity of the hormone for the IR (relative affinity ca. 80%; Table 1A). The variant protein retains a nativelike α-helical moiety with partial or complete disorder between residues B20 and B30. The C-terminal β-strand detaches from the core under acidic conditions (*6*), whereas at neutral pH it remains in part attached (*14*).[7] Alanine, serine, and tyrosine impair receptor binding more significantly (relative affinities 1%, 7%, and ca. 2%, respectively; Table 1) (*13*, *16*, *19*, *79*).[8] Molecular interpretation of these relative affinities is not apparent.

A possible role for Phe^{B24} in redirecting the main chain of insulin on receptor binding has been proposed on the basis of the unexpectedly high activities of D-amino acid substitutions (*12*, *53*). Remarkably, D-Ala, D-Phe, and D-Tyr enhance activity to similar extents (Table 1A), suggesting that it is the main-chain disruption rather than the identity of the side

[7] Ludvigsen and colleagues propose that in Gly^{B24} analogues at neutral pH a structural reorganization takes place in which Phe^{B25} replaces the absent Phe^{B24} in the hydrophobic core, leading to a larger turn (B20−B24) but a similar C-terminal β-strand (*14*). Inspection of their deposited ^{1}H NMR chemical shifts is not in accord with this model as the expected ring-current effects of an internal Phe^{B25} on the neighboring side chain of Leu^{B15} (*75*) are not observed. Reinvestigation of the analogue [Glu^{B16},Gly^{B24}]-insulin at neutral pH suggests an alternative model in which the B24−B30 segment is only partially ordered and in equilibrium between attached and detached conformers (Q. X. Hua and M. A. Weiss, manuscript in preparation). No evidence is obtained for hydrophobic insertion of Phe^{B25} in accord with ring-current analysis of chemical shifts.

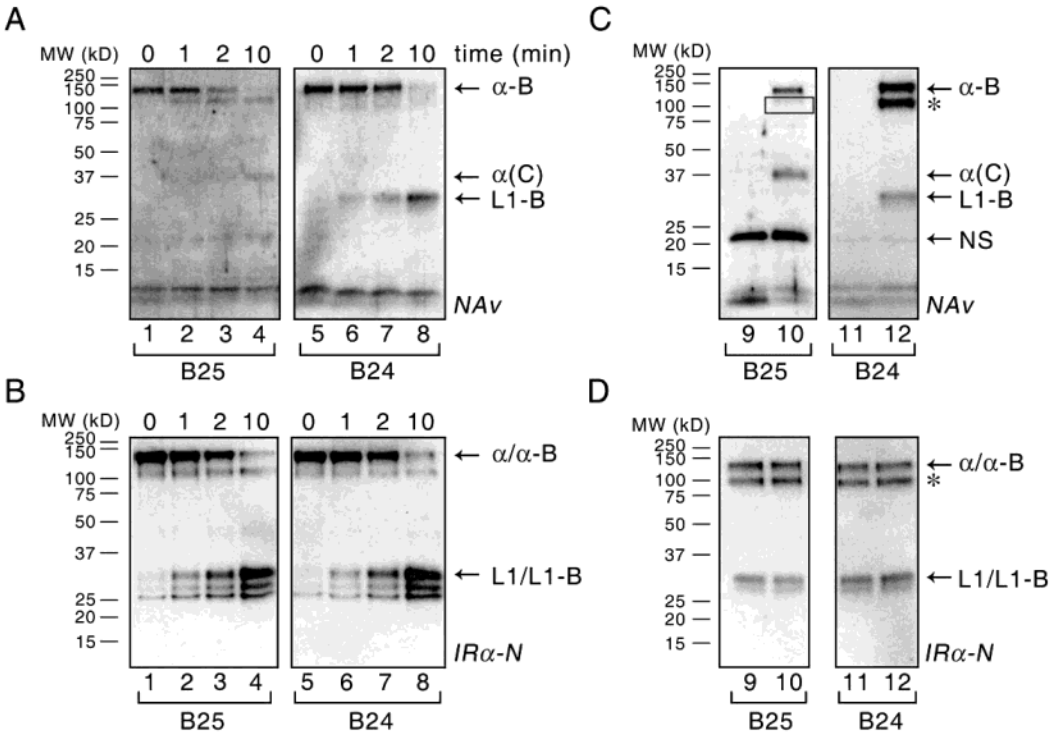

FIGURE 7: Limited trypsin digestion of Pap^{B25}- or Pap^{B24}-cross-linked IR. (A, B) WGA-purified IR was cross-linked to Pap^{B25} or Pap^{B24} derivatives of DKP-insulin and digested with trypsin. At indicated time points (beneath the gels in panels A and B), digestions were stopped by adding soybean trypsin inhibitor. Heat-inactivated and denatured aliquots were resolved by SDS−PAGE and visualized by alkaline phosphatase conjugated NAv (panel A) or IRα-N (panel B). (C and D) Pap^{B25} and Pap^{B24} cross-linking to pretrypsinized insulin receptor. After SDS−PAGE separation and blotting, samples were probed with NAv (C) or anti-IRα antibody (D). α-B designates the covalent complex between the intact α subunit and B-chain analogue. L1−B (apparent molecular mass 31 kDa) designates the covalent complex between the L1 domain and B-chain analogue. In panels A and C, α(C) (apparent molecular mass 37 kDa) designates the fragment containing the carboxy-terminal contact site of Pap^{B25} and the B-chain analogue. Abbreviations are otherwise as in Figure 5.

chain that strengthens receptor binding. The proposed detachment or reorganization of the carboxy-terminal region of the B chain near B24 would expose the side chains of Phe^{B24} and Ile^{A2} and so enable them to engage the receptor (Figure 10A; *13*, *21*). Such an induced fit would also expose the side chains of Ile^{A2} and Val^{A3}, otherwise inaccessible in native structures. Direct contacts between these A-chain residues and the IR would rationalize the exquisite sensitivity of binding to such subtle substitutions as $Ile^{A2} \rightarrow$ *allo*-Ile^{A2} (affinity decreased by 50-fold; *22*) and $Val^{A3} \rightarrow$ Leu (affinity decreased by 500-fold; *54*).

In the crystallographic T state the C-terminal B-chain β-strand not only packs against nonpolar side chains of the A chain but is also tethered by a hydrogen bond between the amide proton of Phe^{B25} and the carbonyl oxygen of Tyr^{A19} (*3*). This hydrogen bond is broken in the R state due to a small displacement of the β-strand (*4*, *49*) and would likewise be expected to be broken on detachment of the strand in the hormone−receptor complex. In an attempt to facilitate such detachment by design, Wollmer and colleagues designed a novel nonstandard analogue in which the B24−B25 peptide bond was replaced by an ester bond (*55*), the first report of replacement of a main-chain atom in insulin. Although meant to enhance activity, loss of the B25−A19 hydrogen bond was associated with impaired activity. Structural studies of the analogue revealed an unexpected gain in hydrophobic interactions achieved by insertion of the Phe^{B25} side chain into the core, shielding this side chain and hindering (rather than facilitating) detachment of the β-strand (*56*). Ascribed to increased rotational freedom of the main chain due to the ester bond, this structural reorganization honors the breach in the detachment model.

The present photo-cross-liking results strongly suggest that Phe^{B24}, like Phe^{B25}, contacts the insulin receptor. It is not clear, however, whether such contacts take place within a native structural context or by means of an altered conformation. Given the structural environment of Phe^{B24} at the edge of the core (Figure 2C), it is likely that in a nativelike structure the azido moiety of Pap^{B24} would project from the surface of the protein even as the remainder of the aromatic side chain is buried in the core. It is also possible that the azido moiety perturbs side chain packing, enhancing its solvent accessibility in the free hormone. Although these possibilities cannot be excluded, we propose that extensive contacts between the IR and Phe^{B24} serve to trigger a conformational change in the C-terminal β-strand, mimicking

[8] Tager and co-workers investigated Tyr^{B24} in the context of an analogue containing substitution $Tyr^{B26} \rightarrow$ Phe (*20*). However, the latter has only a small effect on receptor binding (*20*). We note in passing that the low activity of the Tyr^{B24} analogue is surprising in light of the higher activity of the present Pmp^{B24} analogue (50% relative to the parent biotinylated template). The *p*-hydroxyl function of Tyr exhibits chemical similarities to the *p*-amino function of Pmp, including size, polarity, and potential to donate and receive hydrogen bonds. Because the synthesis of the Tyr^{B24} analogue was not verified by mass spectrometry (*20*), it is possible that effects of this substitution activity should be revisited. Recent reinvestigation of Pmp^{B24} and Tyr^{B24} in the context of despentapeptide[B26−B30]-insulin-amide gave relative activities of 52% and 14%, respectively (S. H. Nakagawa, unpublished results).

effects of D substitutions. In this model the aromatic ring packs within a pocket of the L1 β-helix rather than against the core of the hormone. The details of side chain packing in this pocket could rationalize the otherwise puzzling effects of L-amino acid substitutions (see above). We further suggest that contacts by Phe^{B25} follow secondarily to stabilize this novel conformation. The anomalous effects of substitutions at B24 contrast with consistent structure−activity relationships at B25 (Table 1B), i.e., a straightforward preference for aromatic rings sharing an sp^2-hybridized trigonal carbon at the γ position of the side chain (*15*). Modification of the *para* position of the B25 phenylalanine ring (Pmp or Tyr) does not affect receptor binding. Indeed bulky aromatic side chains such as β-naphthylene are relatively well tolerated, suggesting packing of the side chain over an unrestricted surface or within a large slot. By contrast, diabetes-associated variant Phe^{B25} → Leu (*insulin Chicago*) contains an sp^3-hybridized tetrahedral carbon at the γ position and exhibits a >50-fold reduction in receptor-binding activity (*16*−*18*). Substitution by alanine, glycine, and serine also impairs receptor binding (Table 1B).

Relationship to Previous Cross-Linking Studies. Chemical and photoaffinity cross-linking methods have previously been employed to identify sites of contact between insulin and the IR (for a review, see ref *9*). A chemical cross-linking study identified an amino-terminal 55 kDa chymotryptic fragment (which includes the L1 and CR domains; Figure 3) as containing a major site of insulin binding (*47*). Because chemical cross-linking of native insulin is not residue-specific, efforts have otherwise focused on the design of modified insulins containing specific photoactivatable probes. Two studies utilized azido-based probes to derivatize the ϵ-amino group of Lys^{B29} (*24*, *43*). Discrepant results were obtained (sites of cross-linking were mapped to the L1 domain in one case and tentatively ascribed to the CR domain in the other).[9] Likewise, a photoreactive probe at the amino terminus of the B chain has been shown to contact a fragment spanning residues 390−488 (i.e., carboxy-terminal to the CR domain; *44*). Because sites of photo-cross-linking by probes at B29 and B1 are likely to be peripheral to the hormone−receptor interface and influenced by the flexibility of these terminal segments, Steiner and colleagues focused on Phe^{B25}, which as discussed above is a conserved site in the B-chain β-strand of critical importance for biological activity (*15*). In the context of truncated analogue despentapeptide[B26−B30]-insulin-α-carboxamide, Pap^{B25} cross-links to the carboxy-terminal insert domain of the IR (*10*). Together, these results raise the possibility that regions of the α subunit distant in the sequence are brought into proximity by the overall folding of the receptor.

The present study has extended the approach of Steiner and colleagues (*10*) to employ an aryl azide (Pap) at the preceding residue of the B chain. Unlike B1 and B29, Phe^{B24} and Phe^{B25} are each invariant and contained within the classical binding surface (*3*, *9*, *11*, *57*). The choice of *p*-azidophenylalanine is noteworthy. Although other photoactive reagents have been developed, Pap is closest in shape and size to Phe (or Tyr). Its substitution for Phe^{B24} or Phe^{B25} thereby minimizes steric perturbation to insulin or the receptor complex. Further advantages of Pap derive from its short length and restricted mobility: avoidance of the nonspecific or multiple sites of cross-linking that can be associated with long and flexible tethers. This is of particular significance in the present study. Our goal was to compare short-length cross-linking reagents at contiguous sites in insulin. Fortuitously, this provided a "molecular ruler" with which domain−domain distances in the hormone−receptor complex could be probed. The present characterization of Pap^{B25}-DKP-insulin, although of lower resolution than that of Kurose et al. (based on Edman sequencing; *10*), is nonetheless consistent with the sequence of their cross-linked carboxy-terminal peptide: in the context of an intact insulin analogue Pap^{B25} cross-links within a carboxy-terminal 25 kDa glycosylated fragment (3 kDa B chain of insulin derivation contained) containing the carboxy-terminal tail derived from the insert domain (see the Materials and Methods). By contrast, Pap^{B24}-DKP-insulin cross-links within the amino-terminal L1 domain. To our knowledge, this is the first direct demonstration that the amino-terminal L1 domain and carboxy-terminal tail of the receptor α subunit are in close proximity in the hormone−receptor complex.

Interestingly, contiguity between the amino- and carboxy-terminal domains of the α subunit is in accord with comparative receptor-binding studies of native insulin and a truncated high-affinity analogue, designated X92 (Figure 8; *25*). The analogue lacks the five carboxy-terminal residues of the B chain (B26−B30; *37*).[10] Comparison of intact insulin and X92 enabled the role of the carboxy-terminal segment of the B chain to be probed in the hormone−receptor complex (*25*). Two key substitutions (R14A and H710A) in the IR were observed by Whittaker and colleagues to impair binding of insulin more significantly than binding of X92. Control studies demonstrated that such differential binding was due to the carboxy-terminal truncation of the B chain and not to the substitutions at position A8 or B10 (*25*). Remarkably, one of the alanine substitutions is in the amino-terminal L1 domain (R14A), whereas the other is in the carboxy-terminal tail derived from the insert domain (H710A). Whittaker and colleagues thus proposed that the amino- and carboxy-terminal domains of the receptor each contact the carboxy-terminal region of the B chain—and hence must themselves be in close proximity (*25*). This proposal is strongly supported by the present results.

Structure of the Insulin Receptor. Taken together, cross-linking studies suggest that sites of contact are distributed among noncontiguous segments of the α polypeptide (*10*, *24*, *43*, *44*). Although the structure of the receptor is not known, comparative sequence analysis suggests that the α

[9] The alternative reported sites of photo-cross-linking may be due to the design and location of the probes at a site extrinsic to insulin's receptor-binding surface (*3*, *57*). It is also possible that the proposed CR assignment of Yip and colleagues is in error. The initial assignment of the photolabeled fragment was to the CR domain (obtained on the basis of its reactivity toward an antibody raised to a peptide derived from this domain); sequence analysis was not performed. The assignment was ambiguous, however, as it was also demonstrated that the photolabeled fragment reacts with the antireceptor monoclonal antibodies MA-5, MA-10, and MA-20, which do not bind to the CR domain. Yip and colleagues thus concluded that the photolabeled fragment might alternatively be derived from the region of the α subunit between residues 518 and 633 (*43*).

[10] To enhance activity, the X92 analogue also contained three substitutions (Thr^{A8} → His, His^{B10} → Asp, and Phe^{B25} → Tyr), and the B25 α-carboxylate was amidated (*37*).

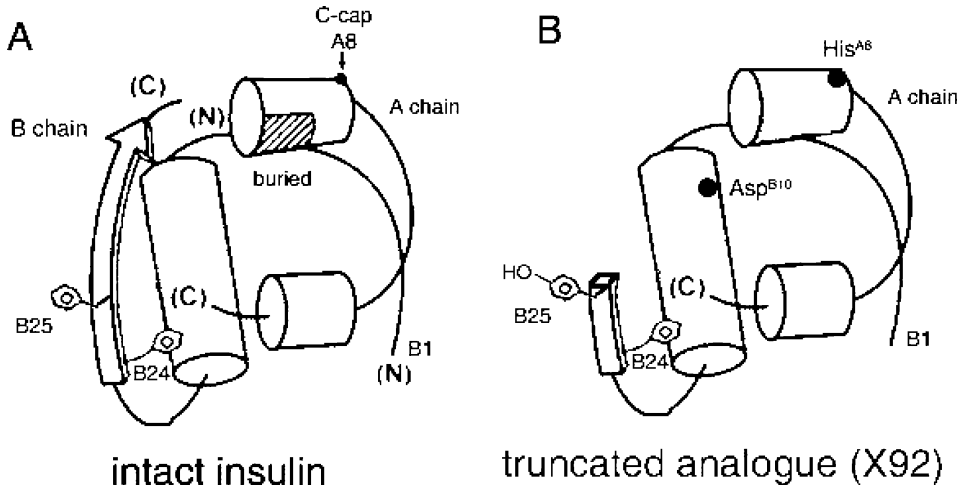

FIGURE 8: Cylinder models of (A) native insulin and (B) X92 truncated analogue (*37*). Structures based on the crystallographic T state (*3*). Residues B24 and B25, sites of present photo-cross-linking, are as indicated. X92 lacks five carboxy-terminal residues of the B chain and contains substitutions Phe^{B25} → Tyr, Thr^{A8} → His, and His^{B10} → Asp; the carboxy terminus of the truncated B chain is amidated. The receptor-binding activity of X92 is ca. 100-fold higher than that of native insulin (*25*, *37*).

subunit consists of a series of modular domains as illustrated in schematic form in Figure 3. Several models of the quaternary organization of the extracellular IR domains have been proposed on the basis of single-molecule EM images (*27*−*32*). Various T-, Y-, X-, U-, bar-, and globular-shaped structures are observed, but their atomic-scale interpretation remains unclear (for reviews, see refs *9* and *58*). An overarching idea is provided by the bivalent model of the insulin−IR complex in which one insulin molecule simultaneously contacts two α subunits. This scheme is reminiscent of how growth hormone and other cytokines bind to their respective receptors (*59*). In addition to its structural elegance, such a model rationalizes the kinetic properties of nonclassical insulin analogues and provides an intuitive mechanism for the complex phenomenon of negative cooperativity (*37*, *60*).

The importance of the L1 domain of the α subunit in conferring high-affinity insulin binding has been highlighted by studies of chimeric receptors (*61*, *62*). The IR and homologous IGF-I receptor (IGF−IR) bind insulin and IGF-I with opposite orders of affinity. Chimeric receptors based on "mixing and matching" domains have thus enabled determinants of ligand specificity to be identified (*63*). In accord with these results, the present study has documented a specific role for the L1 domain in the docking part of the carboxy-terminus β-strand of the insulin B chain. The L1 domain forms a β-helix (Figure 3B), a structural motif shared by otherwise diverse proteins (*64*). Larger than insulin, the L1 β-helix presents both polar and nonpolar surfaces as potential ligand-binding sites. In the absence of structural information a model was proposed (*65*) on the basis of "aromatic complementarity": residues Phe^{B24}, Phe^{B25}, and Tyr^{B26} in insulin were envisaged to interact with aromatic side chains within residues 83−94 of the L1 domain (RGSRL**FF**N**Y**ALV; key aromatic residues in bold). This suggestion was motivated by an analogy between receptor binding and dimerization of insulin (*65*). Those ideas have been refined on the basis of a homology model derived from the crystal structure of the IGF−IR L1−CR−L2 region (*40*). Whittaker and colleagues have defined putative insulin-binding sites on the surface of this model on the basis of alanine scanning mutagenesis: fourteen critical amino acids were identified in four discontinuous segments (*46*). It would be of future interest to define where Phe^{B24} contacts the L1 β-helix in relation to those mutational hot spots and a possible mechanism of aromatic complementarity.

How the L1 β-helix is oriented with respect to the remainder of the IR is not well understood. A Y-shaped model emerged from early studies (*27*−*29*) and has received recent support from a cryo-EM study (Figure 9A; *31*). Image reconstruction of the insulin−holoreceptor complex based on scanning transmission EM has been described at 20 Å resolution (*32*). An atomic-scale interpretation was proposed by Yip and colleagues on the basis of computer-based docking of insulin (based on a crystallographic protomer; Figure 9B) within a putative ligand-binding tunnel between α subunits (*48*). Although this procedure is in part speculative, it is noteworthy that the L1 β-helix emerges as a major insulin-binding surface and in particular that Phe^{B24} is proposed to contact residues Leu87, Phe88, Phe89, and Tyr91, in accord with the aromatic-complementary model of De Meyts (*65*). This and other features of the Yip model will require future testing. Attempts have been made to resolve the domain organization of the IR by single-molecule EM techniques with varying results.

U-shaped models of quaternary organization of the secreted ectodomain have been also proposed on the basis of single-molecule EM images (*30*, *58*). Domain assignments were obtained on the basis of decoration by F_{ab} fragments from anti-IR monoclonal antibodies with known epitopes (Figure 9C). Although these assignments seem well established, it is not clear in such a model how the carboxy-terminal tail of the α subunit might adjoin the L1 domain of either α subunit. To accommodate this structural constraint, we propose a reinterpretation of the U-shaped model (Figure 9D). We envisage that the same overall shape can be partitioned between α subunits not as a side-by-side dimer as originally proposed (Figure 9C; *58*), but instead as interlocked pieces (Figure 9D). This scheme retains the F_{ab}-based assignments of the L1 and L2 domains, but switches their respective assignments to one or the other α subunit. The resulting subunit interface naturally juxtaposes the

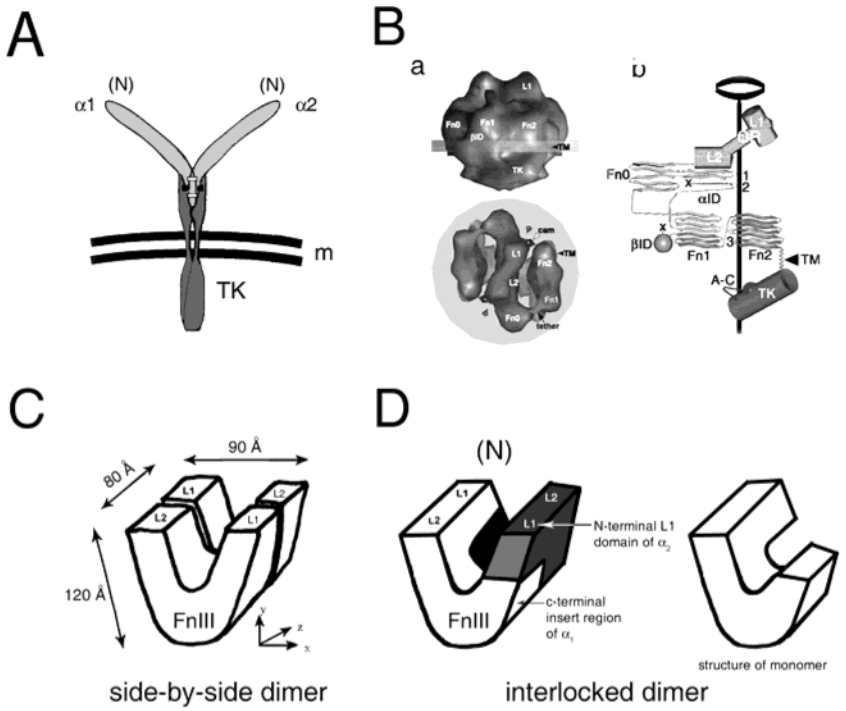

FIGURE 9: EM-derived models of the IR and ectodomain. (A) Y-shaped model of IR based on two-dimensional projection of cryo-EM images (*31*). The IR was solubilized and purified in detergent; similar images were obtained following reconstitution in liposomes. (B) Globular holoreceptor EM image reconstruction (panel a) and proposed domain assignments (panel b) of the hormone−IR complex (*32*, *73*). (C) Side-by-side U-shaped model of secreted ectodomain (*30*). Assignments of L1 and L2 domains were based on binding of F_{ab} fragments. The ectodomain was fixed by glutaraldehyde and stained with uranyl acetate, uranyl formate, potassium phosphotungstate, or methylamine tungstate. (D) A proposed reinterpretation of the U-shaped model in accord with the present results. The same overall U-shape is achieved by interlocked protomers. The proposed shape of teh single protomer is shown at far right. FnIII designates fibronectin-homology regions. The interlocked model is in accord with model 2 in Figure 10B in which Pap^{B24} and Pap^{B25} contact different α subunits.

carboxy-terminal tail of one α subunit near the L1 domain of the other. Such an arrangement predicts in turn that Phe^{B24} and Phe^{B25} themselves bind to different α subunits.

Proximity between the L1 domain and the C-terminal tail of the α subunit is broadly consistent with the design of minimized receptor constructions in which the tail is fused to the end of the L1−CR−L2 region (*26*, *66*). Remarkably, addition of the tail restores hormone binding to the otherwise inactive L1−CR−L2 fragment: insulin is able to bind this construct, albeit with 10-fold lower affinity than to the secreted ectodomain (*26*). In such an engineered complex it is not known how close the tail comes to the L1 domain due to possible domain−domain flexibility within the construct. Irrespective of the details of the structure, this distance is presumably smaller than the diameter of insulin itself. (The orientation of domains observed in the crystal of the IGFR L1−CR−L2 fragment (Figure 3B) may reflect crystal packing rather than the single preferred conformation (*40*).) The functional properties of the monomeric minimized receptor (*26*, *66*) seem to be at variance with the interlocked U-shaped model proposed above. We caution, however, that structure−function relationships in the minimized receptor have not been systematically investigated. It may be that structural features of recognition, including domain−domain relationships, differ from those characteristic of dimeric forms of the α subunit, such as present within the $\alpha_2\beta_2$ holoreceptor.

Concluding Remarks. In the present study two photoactivatable derivatives of insulin, containing respective *p*-azido-phenylalanine substitutions at contiguous positions Phe^{B24} and Phe^{B25}, were synthesized to provide a molecular ruler within an engineered monomer. These positions lie within the classical receptor-binding surface of insulin (*3*) and are sites of mutation causing diabetes mellitus (*11*). On brief ultraviolet irradiation each derivative cross-links efficiently to the insulin holoreceptor and isolated ectodomain. Contacts between Phe^{B24} and the IR may initiate a conformational change in the hormone, exposing a hidden functional surface (*22*). Unexpectedly, our results have demonstrated that the L1 and tail domains of the α subunit are in close proximity in the hormone−receptor complex. Such proximity rationalizes effects of alanine substitutions on binding of a truncated insulin analogue (*25*) and suggests a revised interpretation of electron-microscopic images of the insulin−receptor complex (*58*).

We suggest that on receptor binding the C-terminal β-strand of the B chain detaches from the hydrophobic core to insert between amino- and carboxy-terminal domains of the α subunit of the IR. This model is shown in schematic form in Figure 10. Whereas the free hormone adopts a closed conformation, the bound hormone would expose a hidden functional surface containing Ile^{A2} (Figure 10A). It is not clear whether Phe^{B24} and Phe^{B25} (green and red circles) contact the same α subunit (model 1 in Figure 10B) or different α subunits (model 2). In either case, it would be intriguing if the L1 and tail domains were distant in the free receptor but brought together as a consequence of insulin binding. Because the α subunit is tethered to the β subunits (transmembrane tyrosine kinases) by disulfide bridges, it is possible that such a change in domain−domain distances could alter the structure or orientation of the two β subunits and in turn activate the receptor tyrosine kinase. It will be of great importance to test the present models by high-

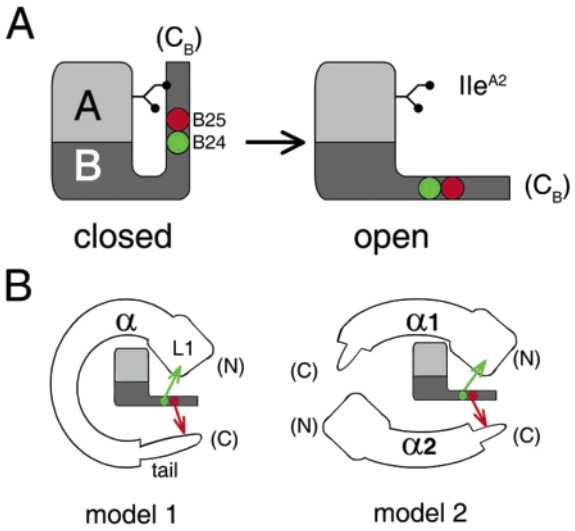

FIGURE 10: Schematic models of insulin and the insulin−IR complex. (A) Model of conformational change of insulin upon receptor binding. Locations of Ile^{A2}, Phe^{B24} (green), and Phe^{B25} (red) are schematically shown. A and B chains are schematically represented as light and dark gray regions. (B) Possible models of insulin receptor in the bound form illustrate the close proximity of the amino-terminal L1 domain and the carboxy-terminal insert domain. In model 1 the amino- and carboxy-terminal domains of each α subunit are in close proximity, whereas in model 2 the amino-terminal domain of one α subunit packs near the carboxy-terminal domain of the other α subunit. The carboxy-terminal tail of the α subunit is derived from the insert domain (see Figure 3A,B).

resolution crystallographic studies of insulin−IR complexes.

ACKNOWLEDGMENT

We thank Prof. D. F. Steiner for the P3-A cell line overexpressing the insulin receptor, Prof. G. D. Smith and C. C. Yip for their gift of purified ectodomain, R.-y. Wang and S. Wang for help with the synthesis, P. De Meyts, L. Schäffer (Novo Research Laboratories), and Q. X. Hua for communication of unpublished results, and G. G. Dodson, P. De Meyts, Q. X. Hua, F. Ismail-Beigi, and M. Snider for helpful discussion.

SUPPORTING INFORMATION AVAILABLE

One figure showing sequence alignment of L1−CR−L2 domains of the insulin receptor and IGF-I receptor (likely tryptic sites and disulfide bridges near the L1−CR junction are highlighted). This material is available free of charge via the Internet at http://pubs.acs.org.

REFERENCES

1. White, M. F., and Kahn, C. R. (1994) The insulin signaling system, *J. Biol. Chem. 269*, 1−4.
2. Blundell, T. L., Cutfield, J. F., Cutfield, S. M., Dodson, E. J., Dodson, G. G., Hodgkin, D. C., Mercola, D. A., and Vijayan, M. (1971) Atomic positions in rhombohedral 2-zinc insulin crystals, *Nature 231*, 506−511.
3. Baker, E. N., Blundell, T. L., Cutfield, J. F., Cutfield, S. M., Dodson, E. J., Dodson, G. G., Hodgkin, D. M., Hubbard, R. E., Isaacs, N. W., and Reynolds, C. D. (1988) The structure of 2Zn pig insulin crystals at 1.5 Å resolution, *Philos. Trans. R. Soc. London 319*, 369−456.
4. Derewenda, U., Derewenda, Z., Dodson, E. J., Dodson, G. G., Reynolds, C. D., Smith, G. D., Sparks, C., and Swenson, D. (1989) Phenol stabilizes more helix in a new symmetrical zinc insulin hexamer, *Nature 338*, 594−596.
5. Badger, J., Harris, M. R., Reynolds, C. D., Evans, A. C., Dodson, E. J., Dodson, G. G., and North, A. C. (1991) Structure of the pig insulin dimer in the cubic crystal, *Acta Crystallogr., Sect. B 47*, 127−136.
6. Hua, Q. X., and Weiss, M. A. (1991) Comparative 2D NMR studies of human insulin and *des*-pentapeptide insulin: sequential resonance assignment and implications for protein dynamics and receptor recognition, *Biochemistry 30*, 5505−5515.
7. Olsen, H. B., Ludvigsen, S., and Kaarsholm, N. C. (1996) Solution structure of an engineered insulin monomer at neutral pH, *Biochemistry 35*, 8836−8845.
8. Hua, Q. X., Hu, S. Q., Frank, B. H., Jia, W., Chu, Y. C., Wang, S. H., Burke, G. T., Katsoyannis, P. G., and Weiss, M. A. (1996) Mapping the functional surface of insulin by design: structure and function of a novel A-chain analogue, *J. Mol. Biol. 264*, 390−403.
9. De Meyts, P., and Whittaker, J. (2002) Structural biology of insulin and IGF−I receptors: implications for drug design, *Nat. Rev. Drug Discov. 1*, 769−783.
10. Kurose, T., Pashmforoush, M., Yoshimasa, Y., Carroll, R., Schwartz, G. P., Burke, G. T., Katsoyannis, P. G., and Steiner, D. F. (1994) Cross-linking of a B25 azidophenylalanine insulin derivative to the carboxyl-terminal region of the alpha-subunit of the insulin receptor. Identification of a new insulin-binding domain in the insulin receptor, *J. Biol. Chem. 269*, 29190−29197.
11. Shoelson, S., Haneda, M., Blix, P., Nanjo, A., Sanke, T., Inouye, K., Steiner, D., Rubenstein, A., and Tager, H. (1983) Three mutant insulins in man, *Nature 302*, 540−543.
12. Mirmira, R. G., and Tager, H. S. (1989) Role of the phenylalanine B24 side chain in directing insulin interaction with its receptor: Importance of main chain conformation, *J. Biol. Chem. 264*, 6349−6354.
13. Hua, Q. X., Shoelson, S. E., Kochoyan, M., and Weiss, M. A. (1991) Receptor binding redefined by a structural switch in a mutant human insulin, *Nature 354*, 238−241.
14. Olsen, H. B., Ludvigsen, S., and Kaarsholm, N. C. (1998) The relationship between insulin bioactivity and structure in the NH2-terminal A-chain helix, *J. Mol. Biol. 284*, 477−488.
15. Mirmira, R. G., and Tager, H. S. (1991) Disposition of the phenylalanine B25 side chain during insulin-receptor and insulin-insulin interactions, *Biochemistry 30*, 8222−8229.
16. Tager, H., Thomas, N., Assoian, R., Rubenstein, A., Saekow, M., Olefsky, J., and Kaiser, E. T. (1980) Semisynthesis and biological activity of porcine [LeuB24]insulin and [LeuB25]insulin, *Proc. Natl. Acad. Sci. U.S.A. 77*, 3181−3185.
17. Nakagawa, S. H., and Tager, H. S. (1986) Role of the phenylalanine B25 side chain in directing insulin interaction with its receptor. Steric and conformational effects, *J. Biol. Chem. 261*, 7332−7341.
18. Shoelson, S. E., Lu, Z. X., Parlautan, L., Lynch, C. S., and Weiss, M. A. (1992) Mutations at the dimer, hexamer, and receptor-binding, surfaces of insulin independently affect insulin-insulin and insulin-receptor interactions, *Biochemistry 31*, 1757−1767.
19. Shoelson, S. E., Lee, J., Lynch, C. S., Backer, J. M., and Pilch, P. F. (1993) BpaB25 insulins. Photoactivatable analogues that quantitatively cross-link, radiolabel, and activate the insulin receptor, *J. Biol. Chem. 268*, 4085−4091.
20. Mirmira, R. G., Nakagawa, S. H., and Tager, H. S. (1991) Importance of the character and configuration of residues B24, B25, and B26 in insulin-receptor interactions, *J. Biol. Chem. 266*, 1428−1436.
21. Derewenda, U., Derewenda, Z., Dodson, E. J., Dodson, G. G., Bing, X., and Markussen, J. (1991) X-ray analysis of the single chain B29-A1 peptide-linked insulin molecule. A completely inactive analogue, *J. Mol. Biol. 220*, 425−433.
22. Xu, B., Hua, Q. X., Nakagawa, S. H., Jia, W., Chu, Y. C., Katsoyannis, P. G., and Weiss, M. A. (2002) Chiral mutagensis of insulin's hidden receptor-binding surface: structure of an *allo*-isoleucineA2 analogue, *J. Mol. Biol. 316*, 435−441.
23. Eberle, A. N., and de Graan, P. N. E. (1985) General principles for photoaffinity labeling of peptide hormone receptors, *Methods Enzymol. 109*, 129−157.
24. Wedekind, F., Baer-Pontzen, K., Bala-Mohan, S., Choli, D., Zahn, H., and Brandenburg, D. (1989) Hormone binding site of the insulin receptor: analysis using photoaffinity-mediated avidin complexing, *Biol. Chem. 370*, 251−258.
25. Mynarcik, D. C., Williams, P. F., Schäffer, L., Yu, G. Q., and Whittaker, J. (1997) Analog binding properties of insulin receptor mutants. Identification of amino acids interacting with the COOH

terminus of the B-chain of the insulin molecule, *J. Biol. Chem. 272*, 2077−2081.
26. Kristensen, C., Wiberg, F. C., Schaffer, L., and Andersen, A. S. (1998) Expression and characterization of a 70-kDa fragment of the insulin receptor that binds insulin. Minimizing ligand binding domain of the insulin receptor, *J. Biol. Chem. 273*, 17780−17786.
27. Christiansen, K., Tranum-Jensen, J., Carlsen, J., and Vinten, J. (1991) A model for the quaternary structure of human placental insulin receptor deduced from electron microscopy, *Proc. Natl. Acad. Sci. U.S.A. 88*, 249−252.
28. Schaefer, E. M., Erickson, H. P., Federwisch, M., Wollmer, A., and Ellis, L. (1992) Structural organization of the human insulin receptor ectodomain, *J. Biol. Chem. 267*, 23393−23402.
29. Tranum-Jensen, J., Christiansen, K., Carlsen, J., Brenzel, G., and Vinten, J. (1994) Membrane topology of insulin receptors reconstituted into lipid vesicles, *J. Membr. Biol. 140*, 215−223.
30. Tulloch, P. A., Lawrence, L. J., McKern, N. M., Robinson, C. P., Bentley, J. D., Cosgrove, L., Ivancic, N., Lovrecz, G. O., Siddle, K., and Ward, C. W. (1999) Single-molecule imaging of human insulin receptor ectodomain and its Fab complexes, *J. Struct. Biol. 125*, 11−8.
31. Woldin, C. N., Hing, F. S., Lee, J., Pilch, P. F., and Shipley, G. G. (1999) Structural studies of the detergent-solubilized and vesicle-reconstituted insulin receptor, *J. Biol. Chem. 274*, 34981−34982.
32. Luo, R. Z., Beniac, D. R., Fernandes, A., Yip, C. C., and Ottensmeyer, F. P. (1999) Quaternary structure of the insulin-insulin receptor complex, *Science 285*, 1077−1080.
33. Barany, G., and Merrifield, R. B. (1980) in *The Peptides* (Gross, E., and Meienhofer, J., Eds.) pp 273−284, Academic Press, New York.
34. Hu, S. Q., Burke, G. T., Schwartz, G. P., Ferderigos, N., Ross, J. B., and Katsoyannis, P. G. (1993) Steric requirements at position B12 for high biological activity in insulin, *Biochemistry 32*, 2631−2635.
35. Weiss, M. A., Hua, Q. X., Lynch, C. S., Frank, B. H., and Shoelson, S. E. (1991) Heteronuclear 2D NMR studies of an engineered insulin monomer: assignment and characterization of the receptor-binding surface by selective ^{2}H and ^{13}C labeling with application to protein design, *Biochemistry 30*, 7373−7389.
36. Weiss, M. A., Hua, Q.-X., Jia, W., Nakagawa, S. H., Chu, Y.-C., Hu, S.-Q., and Katsoyannis, P. G. (2001) Activities of monomeric insulin analogs at position A8 are uncorrelated with their thermodynamic stabilities, *J. Biol. Chem. 276*, 40018−40024.
37. Schäffer, L. (1994) A model for insulin binding to the insulin receptor, *Eur. J. Biochem. 221*, 1127−1132.
38. Herzberg, V. L., Grigorescu, F., Edge, A. S., Spiro, R. G., and Kahn, C. R. (1985) Characterization of insulin receptor carbohydrate by comparison of chemical and enzymatic deglycosylation, *Biochem. Biophys. Res. Commun. 129*, 789−796.
39. Elleman, T. C., Frenkel, M. J., Hoyne, P. A., McKern, N. M., Cosgrove, L., Hewish, D. R., Jachno, K. M., Bentley, J. D., Sankovich, S. E., and Ward, C. W. (2000) Mutational analysis of the N-linked glycosylation sites of the human insulin receptor, *Biochem. J. 347*, 771−779.
40. Garrett, T. P., McKern, N. M., Lou, M., Frenkel, M. J., Bentley, J. D., Lovrecz, G. O., Elleman, T. C., Cosgrove, L. J., and Ward, C. W. (1998) Crystal structure of the first three domains of the type-1 insulin-like growth factor receptor, *Nature 394*, 395−399.
41. Peitsch, M. C. (1996) ProMod and Swiss-Model: Internet-based tools for automated comparative protein modelling, *Biochem. Soc. Trans. 24*, 274−279.
42. Yip, C. C., and Jack, E. (1992) Insulin receptors are bivalent as demonstrated by photoaffinity labeling, *J. Biol. Chem. 267*, 13131−13134.
43. Yip, C. C., Hsu, H., Patel, R. G., Hawley, D. M., Maddux, B. A., and Goldfine, I. D. (1988) Localization of the insulin-binding site to the cysteine-rich region of the insulin receptor alpha-subunit, *Biochem. Biophys. Res. Commun. 157*, 321−329.
44. Fabry, M., Schaefer, E., Ellis, L., Kojro, E., Fahrenholz, F., and Brandenburg, D. (1992) Detection of a new hormone contact site within the insulin receptor ectodomain by the use of a novel photoreactive insulin, *J. Biol. Chem. 267*, 8950−8956.
45. Schumacher, R., Mosthaf, L., Schlessinger, J., Brandenburg, D., and Ullrich, A. (1991) Insulin and insulin-like growth factor-I binding specificity is determined by distinct regions of their cognate receptors, *J. Biol. Chem. 266*, 19288−19295.
46. Williams, P. F., Mynarcik, D. C., Yu, G. Q., and Whittaker, J. (1995) Mapping of an NH2-terminal ligand binding site of the insulin receptor by alanine scanning mutagenesis, *J. Biol. Chem. 270*, 3012−3016.
47. Waugh, S. M., DiBella, E. E., and Pilch, P. F. (1989) Isolation of a proteolytically derived domain of the insulin receptor containing the major site of cross-linking/binding, *Biochemistry 28*, 3448−3455.
48. Yip, C. C., and Ottensmeyer, P. (2003) Three-dimensional structural interactions of insulin and its receptor, *J. Biol. Chem. 278*, 27329−27332.
49. Bentley, G., Dodson, E., Dodson, G., Hodgkin, D., and Mercola, D. (1976) Structure of insulin in 4-zinc insulin, *Nature 261*, 166−168.
50. Ciszak, E., and Smith, G. D. (1994) Crystallographic evidence for dual coordination around zinc in the T3R3 human insulin hexamer, *Biochemistry 33*, 1512−1517.
51. Kobayashi, M., Ohgaku, S., Iwasaki, M., Maegawa, H., Shigeta, Y., and Inouye, K. (1982) Characterization of [LeuB24]- and [LeuB25]-insulin analogues. Receptor binding and biological activity, *Biochem. J. 206*, 597−603.
52. Hua, Q. X., Narhi, L., Jia, W., Arakawa, T., Rosenfeld, R., Hawkins, N., Miller, J. A., and Weiss, M. A. (1996) Native and non-native structure in a protein-folding intermediate: spectroscopic studies of partially reduced IGF−I and an engineered alanine model, *J. Mol. Biol. 259*, 297−313.
53. Kobayashi, M., Ohgaku, S., Iwasaki, M., Maegawa, H., Shigeta, Y., and Inouye, K. (1982) Supernormal insulin: [D-PheB24]-insulin with increased affinity for insulin receptors, *Biochem. Biophys. Res. Commun. 107*, 329−336.
54. Kobayashi, M., Takata, Y., Ishibashi, O., Sasaoka, T., Iwasaki, T. M., Shigeta, Y., and Inouye, K. (1986) Receptor binding and negative cooperativity of a mutant insulin, [LeuA3]-insulin, *Biochem. Biophys. Res. Commun. 137*, 250−257.
55. Wollmer, A., Gilge, G., Brandenburg, D., and Gattner, H. G. (1994) An insulin with the native sequence but virtually no activity, *Biol. Chem. Hoppe-Seyler 375*, 219−222.
56. Kurapkat, G., De Wolf, E., Grotzinger, J., and Wollmer, A. (1997) Inactive conformation of an insulin despite its wild-type sequence, *Protein Sci. 6*, 580−587.
57. Pullen, R. A., Lindsay, D. G., Wood, S. P., Tickle, I. J., Blundell, T. L., Wollmer, A., Krail, G., Brandenburg, D., Zahn, H., Gliemann, J., and Gammeltoft, S. (1976) Receptor-binding region of insulin, *Nature 259*, 369−373.
58. Adams, T. E., Epa, V. C., Garrett, T. P. J., and Ward, C. W. (2000) Structure and function of the type 1 insulin-like growth factor receptor, *Cell Mol. Life Sci. 57*, 1050−1093.
59. de Vos, A. M., Ultsch, M., and Kossiakoff, A. A. (1992) Human growth hormone and extracellular domain of its receptor: crystal structure of the complex, *Science 255*, 306−312.
60. De Meyts, P. (1994) The structural basis of insulin and insulin-like growth factor-I receptor binding and negative co-operativity, and its relevance to mitogenic versus metabolic signalling. *Diabetologia 37* (Suppl. 2), S135−S148.
61. Andersen, A. S., Kjeldsen, T., Wiberg, F. C., Vissing, H., Schaffer, L., Rasmussen, J. S., De Meyts, P., and Moller, N. P. (1992) Indentification of determinants that confer ligand specificity on the insulin receptor, *J. Biol. Chem. 267*, 13681−13686.
62. Schumacher, R., Soos, M. A., Schlessinger, J., Brandenburg, D., Siddle, K., and Ullrich, A. (1993) Signaling-competent chimeras allow mapping of major insulin receptor binding domains determinants, *J. Biochem. 268*, 1087−1094.
63. Kjeldsen, T., Andersen, A. S., Wiberg, F. C., Rasmussen, J. S., Schaffer, L., Balschmidt, P., Moller, K. B., and Moller, N. P. H. (1991) The ligand specificities of the insulin receptor and the insulin-like growth factor I reside in different regions of a common binding site, *Proc. Natl. Acad. Sci. U.S.A. 88*, 4404−4408.
64. Kobe, B., and Deisenhofer, J. (1995) Proteins with leucine-rich repeats, *Curr. Opin. Struct. Biol. 5*, 409−16.
65. De Meyts, P., Gu, J. L., Shymko, R. M., Kaplan, B. E., Bell, G. I., and Whittaker, J. (1990) Identification of a ligand-binding region of the human insulin receptor encoded by the second exon of the gene, *Mol. Endocrinol. 4*, 409−416.
66. Molina, L., Marino-Buslje, C., Quinn, D. R., and Siddle, K. (2000) Structural domains of the insulin receptor and IGF receptor required for dimerisation and ligand binding, *FEBS Lett. 467*, 226−230.
67. Keefer, L. M., Piron, M. A., De Meyts, P., Gattner, H. G., Diaconescu, C., and Brandenburg, D. (1981) Impaired negative

cooperativity of the semi-synthetic analogues human (LeuB24)- and (LeuB25)-insulins, *Biochem. Biophys. Res. Commun. 100*, 1229−1236.

68. Jonczyk, A., Keefer, L. M., Naithani, V. K., Gattner, H. G., De Meyts, P., and Zahn, H. (1981) Preparation and biological properties of [LeuB24, LeuB25]human insulin, *Hoppe-Seyler's Z. Physiol. Chem. 362*, 557−561.
69. Kobayashi, M., Haneda, M., Maegawa, H., Watanabe, N., Takada, Y., Shigeta, Y., and Inouye, K. (1984) Receptor binding and biological activity of [SerB24]-insulin, an abnormal mutant insulin, *Biochem. Biophys. Res. Commun. 119*, 49−57.
70. Inouye, K., Watanabe, K., Tochino, Y., Kanaya, T., Kobayashi, M., and Shigeta, Y. (1981) Semisynthesis and biological properties of the [B24-leucine]-, [B25-leucine]- and [B24-leucine, B25-leucine]-analogues of human insulin, *Experientia 37*, 811−813.
71. Mynarcik, D. C., Yu, G. Q., and Whittaker, J. (1996) Alanine-scanning mutagenesis of a C-terminal ligand binding domain of the insulin receptor alpha subunit, *J. Biol. Chem. 271*, 2439−2442.
72. Marino-Buslje, C., Martin-Martinez, M., Mizuguchi, K., Siddle, K., and Blundell, T. L. (1999) The insulin receptor: from protein sequence to structure, *Biochem. Soc. Trans. 27*, 715−726.
73. Ottensmeyer, F. P., Beniac, D. R., Luo, R. Z., and Yip, C. C. (2000) Mechanism of transmembrane signaling: insulin binding and the insulin receptor, *Biochemistry 39*, 12103−12112.
74. Mynarcik, D. C., Williams, P. F., Schäffer, L., Yu, G. Q., and Whittaker, J. (1997) Identification of common ligand binding determinants of the insulin and insulin-like growth factor 1 receptors. Insights into mechanisms of ligand binding, *J. Biol. Chem. 272*, 18650−18655.
75. Jacoby, E., Hua, Q. X., Stern, A. S., Frank, B. H., and Weiss, M. A. (1996) Structure and dynamics of a protein assembly. 1H-NMR studies of the 36 kDa R6 insulin hexamer, *J. Mol. Biol. 258*, 136−157.
76. Xu, b., Hu, S-Q., Chu, Y-C., Wang, S., Wang, R.-y., Nakagawa, S. H., and Weiss, M. A. (2004) Diabetes-associated mutations in insulin identify invariant receptor contacts, *Diabetes. 53*, 1599−1602.

BI0497796